Trends in Analytical Chemistry 180 (2024) 117972

Contents lists available at ScienceDirect

Trends in Analytical Chemistry

journal homepage: www.elsevier.com/locate/trac

Strategies for enhancing the selectivity of quantum dot-based fluorometric methods

Rodolfo M.M. Santana [a,*], Leila S.V. Barbosa [a], Leandro G. Benzi [a], Rafael C. Castro [b], David S.M. Ribeiro [b], Maria Graças A. Korn [a,c], João L.M. Santos [b,**], Leonardo S.G. Teixeira [a,c,***]

[a] Federal University of Bahia, Chemistry Institute, Analytical Chemistry Department, Campus Universitário de Ondina, 40170-115, Salvador, Bahia, Brazil
[b] LAQV, REQUIMTE, Department of Chemical Sciences, Laboratory of Applied Chemistry, Faculty of Pharmacy, University of Porto, Rua de Jorge Viterbo Ferreira, n° 228, Porto, 4050-313, Portugal
[c] INCT de Energia e Ambiente - Universidade Federal da Bahia, Instituto de Química, Campus Universitário de Ondina, 40170-115, Salvador, Bahia, Brazil

ARTICLE INFO

Keywords:
Quantum dots
Selectivity
Sensing
Surface modification
Sample preparation
Chemometric models

ABSTRACT

In recent decades, quantum dots (QDs) have emerged as highly efficient fluorophores, enabling the quantification of various species across diverse fields. However, their typically unspecific sensing mechanisms, arising from their high reactivity and propensity to establish nonspecific interactions, frequently lead to a lack of selectivity, which hinders their application in the analysis of complex samples. This review presents the state-of-the-art of the most commonly applied QD-based analytical approaches to circumvent these limitations and improve selectivity. Moreover, several interesting examples of surface modification, sample preparation, and chemometric tools are highlighted to demonstrate their potentialities and shortcomings. This review profiles the trends and perspectives to broaden the analytical application of QDs.

Abbreviations

[BMIM][BF4]	1-Butyl-3-methylimidazolium tetrafluoroborate	LLME	Liquid–liquid microextraction
[BMIM][Br]	1-Butyl-3-methylimidazolium bromide	MAA	Methacrylic acid
AIBN	Azobisisobutyronitrile	MCR-ALS	Multivariate curve resolution-alternating least squares
AM	(Aminomethyl)	MIP	Molecularly printed polymers
ANN	Artificial neural network	MNP	Magnetic nanoparticles
APTES	(3-Aminopropyl) triethoxysilane	MP	Magnetic particles
BSA	Bovine serum albumin	MPA	Mercaptopropionic acid
CD	Carbon dots	MSPE	Magnetic solid-phase extraction
CPE	Cloud point extraction	N-CD	Nitrogen-doped carbon dots
CYS	L-Cysteine	NP	Nanoparticles
EEM	Excitation–emission matrix	OTC	Oxytetracycline
EGDMA	Ethylene glycol dimethylacrylate	PCA	Principal component analysis
ET	Electron transfer	PL	Photoluminescence
F-CD	Fluorine-doped carbon dots	PLS	Partial least squares
FRET	Fluorescence resonance energy transfer	POSS	Polyhedral oligomeric silsesquioxanes
GOQD	Graphene oxide quantum dots	QD	Quantum dots
GQD	Graphene quantum dots	R_2CV	Coefficient of determination of cross-validation
GSH	Glutathione	S-CD	Sulfur-doped carbon dots
HG	Hydride generation	SPE	Solid-phase extraction
HG-SPE	Hydride generation solid phase extraction	TEOS	Tetraethylorthosilicate
HS-SDME	Headspace single-drop microextraction	TGA	Thioglycolic acid

(continued on next column)

(continued)

(continued on next page)

* Corresponding author.
** Corresponding author.
*** Corresponding author. Federal University of Bahia, Chemistry Institute, Analytical Chemistry Department, Campus Universitário de Ondina, 40170-115, Salvador, Bahia, Brazil
E-mail addresses: rodolfo.magalhaes@ufba.br, rodolfommsantana@gmail.com (R.M.M. Santana).

https://doi.org/10.1016/j.trac.2024.117972
Received 17 July 2024; Received in revised form 11 September 2024; Accepted 13 September 2024
Available online 14 September 2024

(*continued*)

IIP	Ion imprinted polymers	TMA	Thiomalic acid
IL	Ionic liquid	UA-TIL-DLLME	Ultrasound-assisted dispersive liquid–liquid microextraction with ionic liquid
LLLME	Liquid–liquid–liquid microextraction	VA-LLME	Vortex-assisted liquid–liquid microextraction

1. Introduction

Analytical methodologies relying on the photoluminescence (PL) properties of chemical species have been applied in the determination of organic, inorganic and biomolecules analytes because of their characteristics such as simplicity, ease of operation, and sensitivity [1,2]. However, the reduced number of existing fluorophores, either native fluorescent analytes prone to direct detection or fluorescent sensing probes suited for indirect analyte determination, has been a remarkable hindrance to expanding the applicability of PL measurements [3,4]. This scenario was modified in the past forty years, when quantum dots (QDs) were identified as promising nanomaterials for different purposes, exhibiting operational versatility that ranges from photonics to electronic devices or (bio)chemical applications, for example, as florescent probes in analytical sensing [5]. The PL of the QD probe can be quenched or enhanced by various inorganic species and organic molecules, a modulation process that is related mainly to their surface states [6,7].

The extensive use of QDs for the development of analytical methods is related to their physical and optical properties, which offer a range of advantages over organic fluorophores, such as straightforward fine-tuning of the emission wavelength through control of the nanocrystal size; high photostability, photosensitivity and photoluminescence; high quantum yield; and the possibility of adjusting their surface chemistry to enable, for example, molecular recognition mechanisms. In the past 15 years, more than 130,000 publications in different research areas mentioned the term “quantum dots”. Considering only “analytical chemistry”, the number of publications that use QDs has been increasing, resulting in more than 11,000 publications.

In general, the low detection limits achieved, wide linear response range, instrumental simplicity and low maintenance and analysis costs, compared with those of other analytical methods, are highlighted for QD-based methods. From the perspective of the matrix samples, water [8], food [9], pharmaceutical [10,11], environmental [12], and biological [13,14] stand out. However, aqueous media (*i.e.*, water samples or dissolved samples in dilute aqueous solutions) have been the most used samples for evaluating the applicability of QD methods because their matrix is simpler than that of other samples, especially organic samples. Another important aspect is that most of these employed nanoparticles are hydrophilic.

Review articles covering distinct analytical aspects, such as the use of QDs for the determination of inorganic species [15,16], including anion [17] detection of pesticides [18] and food contaminants [19] and bioanalytical [20,21] applications, have been published. Among the numerous species and applications, the predominance of aqueous matrix or synthetic samples for QD method validation and application should be highlighted [22–24]. Presumably, the QD-sensing mechanisms were the underlying motive of this practice. The QD response occurs through surface phenomena such as charge carrier transfer like electron transfer (ET) or hole transfer (HT), fluorescence resonance energy transfer (FRET), and changes in the surface–ligand charge or passivation [25,26]. All these processes lack selectivity and are strongly affected by the matrix composition. In this context, different strategies have been explored to circumvent selectivity issues and extend the range of analytical applications of QDs. These strategies include the modification of the QD surface or structure; extraction strategies, including the use of microdevices; the combination of multiple probes, molecularly printed polymers (MIPs), and ionic liquids (ILs) as surface binders; and the use of chemometric tools for data analysis.

In this overview, the different strategies that could be used to enhance the selectivity of QD-based fluorometric methods are discussed, along with the challenges and perspectives that they raise, as well as the future trends and prospects on this topic.

2. Analytical strategies for enhancing the selectivity of QD-based fluorometric methods

2.1. QD synthesis and surface modification

Different methods can be applied to synthesize QDs, affecting the presence of impurities, crystallinity, shape, and size of the resulting nanoparticles and consequently influencing their properties. Modifications can be made to the synthesis route to improve its application [27,28]. In this way, the synthesis method selection can be used to control the properties of the QDs by tuning the operational parameters of the synthesis [29].

Nanocrystal size, for example, influences the photochemical properties of QDs because of the effects of quantum size and variations in the surface area-to-volume ratio [30]. These variations can affect the magnitude of fluorescence and QD reactivity, influencing selectivity. The parameters of the reactional system can be modified to control the nanoparticle size with a posterior evaluation of how each obtained size dictates the QD selectivity toward the target species. The size-dependent electronic and optical properties of QDs arise from quantum confinement effects [31], which dictate nanoparticle reactivity. The effect of particle size on the selectivity of CdTe QDs, for example, was studied for the determination of Hg(II) [32]. The proposed probe was based on the decrease in fluorescence of the QD, which was previously linked, on its surface, to bovine serum albumin (BSA). In the hydrothermal synthesis method [33], the time of heating reflux at different temperatures was varied, and QDs with well-tuned fluorescence wavelengths were obtained. Nanoparticles of different sizes (from 1.98 to 3.68 nm) were prepared, changing the wavelength of the fluorescence emission from 518 to 620 nm. The selectivity of the proposed probe improved as the size of the BSA-coated CdTe QDs decreased: green fluorescent QDs were more selective than red fluorescent QDs, allowing for Hg(II) determination. The impact of nanoparticle size on selectivity can also be exemplified in the determination of uranyl ions by CdTe QDs [34]. The QD size is a critical parameter for selectivity; among the four different QDs synthesized (2.3, 3.1, 5.2, and 6.8 nm), the smallest QDs presented greater quenching for different metal species than did uranyl. The 6.8 nm CdTe QDs exhibited pronounced quenching in the presence of uranyl, whereas the other ions had few effects on the fluorescence emission (Fig. 1a).

Another strategy for improving the selectivity of QD-based methods is via surface-engineered quantum dots via electron transfer pathway manipulation (Fig. 1b). For the CdS:Mn/ZnS QDs, for example, various metal ions promote luminescence quenching of the nanoparticles, making the determination of a specific metallic ion with analytical application difficult [35]. However, the modification of the QD surface upon attachment of 1,10-diaza-18-crown-6 via zero-length covalent coupling allowed the selective determination of Cd(II). Following this modification, CS_2 could be linked and coupled onto the QD surface and to the ligand. In general, the use of a capping agent in a synthetic pathway is concurrent with the QD nucleation process, promoting colloid stabilization and inhibiting uncontrolled agglomeration and growth of the nanoparticles. The presence of the ligand can control, in addition to the growth rate and morphology [36], the solubility, size and reactivity of the nanoparticle, thus affecting selectivity. In this sense, the photophysical properties of QDs can be modulated through photoinduced electron and energy transfer processes between the nanoparticle and the attached ligand to respond to a given chemical stimulus [37].

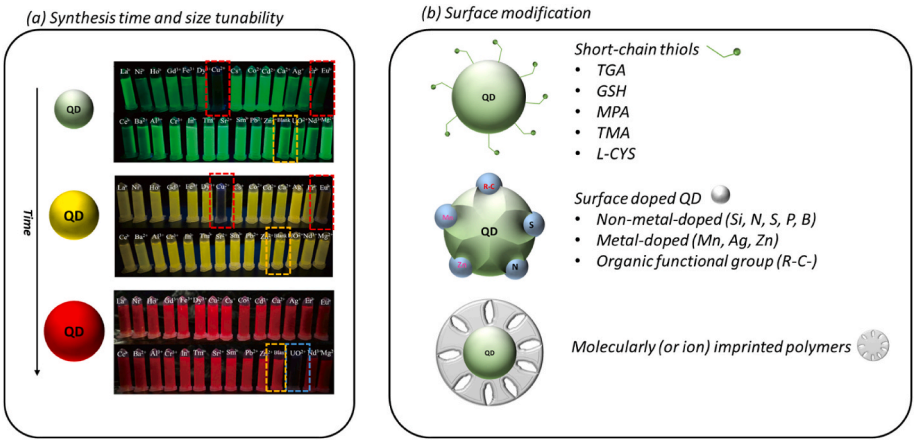

Fig. 1. Strategies of QD synthesis to improve method selectivity (a) QD size effect on the selectivity sensing of Uranyl (—) and potential interferences (—) by qhenching (— Blank). Adapted with permission from Ref. [34] Copyright 2018 Elsevier Publications. (b) Typical surface modifications of QD as analytical fluorophore.

A trivial example, which is used to improve the performance of QDs as nanoprobes in aqueous media, is the functionalization of the surface of these nanocrystals with short-chain thiol ligands. Mercaptopropionic acid (MPA), thioglycolic acid (TGA), glutathione (GSH) and L-cysteine (CYS) are used as capping molecules because they can bind to the core (nucleus) of the QD through the thiol group. To demonstrate the importance of the presence of a ligand in the selectivity of a QD, a systematic study using a CdS QD as a luminescent ion probe is needed [38]. Synthesis in aqueous media obtained water-soluble CdS QDs capped with thioglycerol, L-cysteine, and polyphosphate. The ligand type strongly influenced the response of the nanoparticle toward different metallic cations. The quantum dots capped with polyphosphate showed no selective response and were sensitive to the presence of various ions (mono- and divalent cations). In contrast, the QDs capped with thioglycerol responded only to the presence of iron and copper ions, whereas the QDs capped with L-cysteine responded to zinc ions and were insensitive to other cations, such as calcium, magnesium, and copper. The interaction mechanism is also modified depending on the ligand [39]: CYS-capped CdS QD fluorescence emission increases with increasing zinc ion concentration, whereas thioglycerol-capped CdS QD fluorescence emission is quenched with increasing copper ion concentration [38].

Similarly, liquid ionic (IL)-based carbon dots synthesized under microwave radiation showed unambiguous selectivity for different inorganic ions when only the IL anions were changed. The authors used 1-butyl-3-methylimidazolium bromide ([BMIM][Br]) and 1-butyl-3-methylimidazolium tetrafluoroborate ([BMIM][BF_4]), which, under microwave irradiation, led to the formation of N-doped carbon dots with distinct surface compositions. The anions Br^- and $[BF_4]^-$ have a distinctive radius and ionic conductivity, modifying the IL polarity and thus altering all ionic–microwave interactions. Thus, the obtained nitrogen-doped carbon dots were rich in imidazole groups ([BMIM][Br]) at the surface, whereas the ([BMIM][BF_4]) dots were hydroxyl-containing. These surface characteristics induced preferential interactions with Cu^{2+} (by N-imidazole chelation) or with Fe^{3+} (by high binding hydroxyl affinity) and good selectivity over other metal ions [40].

Molecularly imprinted polymers (MIPs) are notorious materials correlated with selectivity gain because they can mimic the binding sites of target molecules (templates). MIP synthesis is low-cost and relatively simple, and the resulting material is thermally and chemically stable. These characteristics combined with the QDs allowed the production of intrinsically selective luminescent probes (QD@MIPs), which have been extensively applied to develop analytical methods. Typically, silicon polymers prepared with (3-aminopropyl)triethoxysilane (APTES) and tetraethylorthosilicate (TEOS) were adopted to synthesize QD@MIP since this material presents low UV–Vis interactions. In this way, the QD PL properties remain practically unaffected after the formation of the composite [41].

Compared with nonmodified QDs, the QD@MIP composite has shown great selectivity for many species in different samples (Table 1). Even considering compounds with structural similarity to tetracycline antibiotics, a certain gain in selectivity was observed [42]. For oxytetracycline (OTC) determination in honey samples via biomass carbon dots (CDs) associated with MIPs, chlortetracycline and tetracycline fit OTC MIP cavities and could quench the QD PL. However, the higher MIP-OTC affinity ensures preferential interactions and accurate results. Importantly, nonmodified CDs presented comparable PL quenching when exposed to these three tetracyclines, which proves the effect of the MIP on method selectivity. Likewise, the simultaneous determination of cephalexin and ceftriaxone using an optosensor with two QD@MIPs has been successfully applied to milk analysis. The potential interfering species have remarkably similar structures; for example, cefadroxil contains only an additional p-hydroxyl group in the benzene ring, and even so, the generated cavity is selective for cephalexin.

The use of ion-imprinted polymers (IIPs) with QDs has rarely been reported. The ionic imprinting technique is similar to molecular printing, in which an ionic metal (or metal complex) is used as a template [43,44]. However, IIP@QD composites were prepared via direct ionic metal–monomer complexation [45–49]. In this synthetic route, Cu(II) determination in environmental water via a paper microdevice containing the IIP@TGA-CdTe composite resulted in good selectivity [47]. The determination of Cr(VI) via silanized IIP@Mn:ZnS showed greater selectivity for Cr(VI), but there were also considerable changes in the probe fluorescence in the presence of some ions, such as sulfate, phosphate and molybdate, which have similar spatial structures [49]. Although the selectivity can be improved by surface modification, QD particles could be deeply affected by the medium composition owing to structural and charge alterations. In this sense, controlling the media of the PL probe plays an important role in ensuring proper analytical selectivity.

2.2. Control of the reaction medium conditions

When an analytical method based on the use of QDs as a fluorescent probe is established, the reaction conditions need to be studied to find the best conditions for determination. For this purpose, parameters such as pH, ionic strength, the QD concentration, the type of buffer solution, and the presence of auxiliary reagents are generally evaluated. Among these parameters, pH and the presence of a masking agent have a special

Table 1
QD-imprinted polymer composites and their applications for selectivity method development.

Quantum dot	Polymer precursors	Template	Sample	Potential interferents tested	LOD	LOQ	Ref.
TGA-CdTe	Monomer: APTES Cross-linker: TEOS Catalyst: NH_4OH 25 %	Amoxicillin	Egg, milk, honey	Ampicillin, cephalexin, penicillin G, chloramphenicol, thiamphenicol	0.14 μg L^{-1}	0.46 μg L^{-1}	[50]
CYS-CdSe/ZnS	Monomer: APTES Cross-linker: TEOS Catalyst: NH_4OH	Acetaminophen	Tap and river water	L-Ascorbic acid, epinephrine, dopamine, L-DOPA, 4-aminophenol, ketoprofen, sodium diclofenac, sulfamethoxazole, tryptophan, estradiol, uric acid	n.a	n.a	[51]
Si:CD	Monomer: APTES Cross-linker: TEOS Catalyst: NH_4OH 25 %	Caffeic acid	Blood plasma	Na^+, Ca^{2+}, Mg^{2+}, glucose, galactose, glycin, cysteine, albumin	19.8 μg L^{-1}	n.a	[52]
Si:GQD and TGA-CdTe	Monomer: APTES Cross-linker: TEOS Catalyst: NH_4OH 25 %	Cephalexin[a] and Ceftriaxone[b]	Milk	Cefixime, ceftazidime, cefadroxil	0.06[a] and 0.10 b μg L^{-1}	0.20[a] and 0.32 b μg L^{-1}	[53]
N:CD	Monomer: MAA Cross-linker: EGDMA Catalyst: AIBN	3-Monochloropropane-1,2-diol	Soy sauce	Ethylene glycol, glycerol, 1,2-propanediol, 1,3-dichloro-2-propanol, 2,3-dichloro-1-propanol	0.6 μg L^{-1}	n.a	[54]
CdTe@CdS-TGA	Monomer: APTES Cross-linker: TEOS Catalyst: NH_4OH 25 %	Perfluorooctanoic acid	Water	Perfluorooctane sulfonate, SDS, SDBS	10.35 μg L^{-1}	n.a	[55]
Si:CD	Monomer: APTES Cross-linker: TEOS Catalyst: NH_4OH	Oxytetracycline	Honey	Chlortetracycline, tetracycline	15.3 μg L^{-1}	n.a	[42]
CD	Monomer: APTES Cross-linker: TEOS Catalyst: NH_4OH 25 %	Phenobarbital	Blood plasma	Dopamine, ascorbic acid, tryptophan, glucose, cysteine, primidone, K^+, Mg^{2+}, uric acid, glutathione, Adrenaline, histamine, ibuprofen, epinephrine, tryptamine	0.023 μg L^{-1}	n.a	[56]
MPA-CdTe	Monomer: APTES Cross-linker: TEOS Catalyst: NH_4OH	Sulfadiazine	Seawater	Sulfamethazine, sulfamerazine, Sulfamonomethoxine, sulfamethoxazole, ciprofloxacin, erythromycin	167.6 μg L^{-1}	n.a	[57]
TGA-CdTe	Monomer: APTES Cross-linker: TEOS	p-Coumaric acid	Pineapple and kiwi juice	Ferulic acid, caffeic acid, cinnamic acid, chlorogenic acid, 4-hydroxybenzoic acid, vanillic acid	6.74 μg L^{-1}	22.23 μg L^{-1}	[58]
Mn:ZnS@SiO_2	Monomer: AAPTS Cross-linker: TEOS	Cr(VI)	Tap water, lake water and industrial wastewater	Cr^{3+}, Cu^{2+}, Cl^-, SO_4^{2-}, MoO_4^{2-}	5.48 μg L^{-1}	n.a	[49]
Si:CD	Monomer: APTES Cross-linker: TEOS Catalyst: NH_4OH	Acetamiprid	Wastewater and apple	Imidacloprid, indoxacarb, chlorpyrifos, fenitrothion, dichlorvos, difenoconazole	0.45 μg L^{-1}	n.a	[59]
Si:GQD@Fe_3O_4	Monomer: APTES Cross-linker: TEOS	Ceftazidime	Milk	ceftriaxone, cefadroxil, cephalexin, cefazolin	0.05 μg L^{-1}	n.a	[60]

(*continued on next page*)

Table 1 (*continued*)

Quantum dot	Polymer precursors	Template	Sample	Potential interferents tested	LOD	LOQ	Ref.
Si:GQD	Catalyst: NH_4OH Monomer: MAA Cross-linker: EGDMA Catalyst: AIBN	Methamphetamine	None	amphetamine, ibuprofen, codeine, morphine	1.7 μg L^{-1}	n.a	[61]
ZnSe-TGA	Monomer: APTES Cross-linker: TEOS Catalyst: NH_4OH	Cd^{2+} and Pb^{2+}	Lake water, Seawater	Co^{2+}, Cu^{2+}, Hg^{2+}, Ni^{2+}	0.245 μg L^{-1} and 0.335 μg L^{-1} for Cd^{2+} and Pb^{2+}, respectively	n.a	[48]
Mn:ZnS@SiO_2	Monomer: AM and POSS Cross-linker: EGDMA Catalyst: AIBN	Paclitaxel	None	Docetaxel, etoposide, 10-deacetylbaccatin	36.7 μg L^{-1}	n.a	[62]
SiO_2@Mn:ZnS-TGA@Fe_3O_4	Monomer: APTES Cross-linker: TEOS Catalyst: NH_4OH	Norfloxacin	Fish and Milk	Enrofloxacin, ofloxacin, sulfadiazine, trimethoprim, cephalexin, amoxicillin	<0.80 μg L^{-1}	n.a	[63]
Si:CD	Monomer: APTES Cross-linker: TEOS Catalyst: NH_4OH	S-Naproxen and R-Naproxen	Naproxen Tablet	citalopram, propranolol, ibuprofen, Fe^{2+}, Cu^{2+}, Zn^{2+}, Na^{+}, K^{+}	46.1 and 85.2 μg L^{-1} for S- and R-naproxen, respectively	n.a	[64]
Si:CD	Monomer: APTES Cross-linker: TEOS Catalyst: NH_4OH	Indoxacarb	Water, Apple, Tomato	difenoconazole, imidacloprid, dichlorvos, fenitrothion, acetamiprid, chlorpyrifos	0.53 μg L^{-1}	n.a	[41]
Si:CD	Monomer: APTES Cross-linker: TEOS Catalyst: NH_4OH	Microcystin-LR	Lake Water, Tap Water	Microcystin-RR, microcystin-YR	0.0093 μg L^{-1}	n.a	[46]
Mn:ZnS and GQD@SiO_2	Monomer: APTES Cross-linker: TEOS Catalyst: NH4OH	Sinapic Acid	Semen sinapis, Descurainiae semen	HCO_3^-, SO_4^{2-}, Cl^-, $H_2PO_4^-$, K^+, Na^+, Ca^{2+}, Mg^{2+}, Mn^{2+}, Zn^{2+}, Ag^+, Fe^{3+}, chlorogenic acid, oleanonic acid, vanillic acid, *trans*-cinnamic acid, ascorbic acid	0.19 μg L^{-1}	n.a	[65]

n.a: non-available.

influence on the selectivity of the method (Fig. 2).

pH considerably alters the optical properties of QDs because, depending on pH, both the structure of the QD and the surface binder can be altered. In general, QD-based systems present luminescent stability at pH values ranging from 7 to 12. When thiol ligands are present, for example, pH values below 5 can lead to protonation of the functional groups, leading to fluorescence suppression due to the detachment of these ligands from the QD surface. In addition, agglomeration of the QDs and degradation of the nanomaterial due to the formation of hydroxy complexes led to quenching effects at pH values greater than 12.

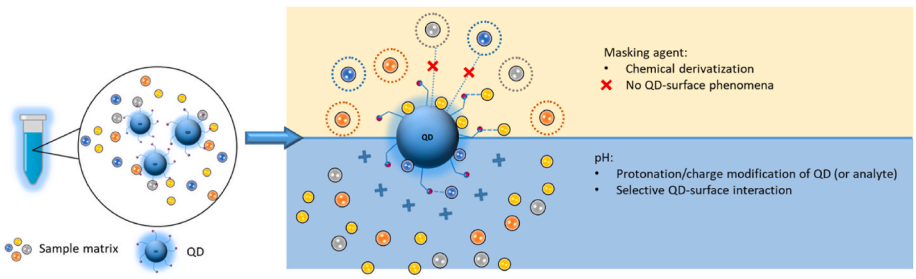

Fig. 2. Scheme of probe composition effect on QD selective sensing by adding masking agents and pH control.

The improved selectivity achieved by pH tuning can be exemplified by determining Cr(III) with yellow fluorescent carbon quantum dots (y-CDs). The nanoparticle fluorescence was pH independent between pH 4.0 and 11.4. However, the presence of several cations quenches y-CD emission under conditions of near-neutral pH. The condition for selectively determining Cr(III) was found at pH 4, in which the fluorescence was affected only by this species [66]. The strategy of pH tuning can also be applied to the determination of organic species. The interactions of glutathione-capped CdTe quantum dots (GSH-CdTe QDs) with heme-containing proteins were studied over a wide pH range, and distinct fluorescence depending on the pH and protein species was observed. The selective determination of cytochrome *c* was possible at pH $>$ 8 since only this protein quenches QD fluorescence. For other proteins, including hemoglobin, the fluorescent signal remained unchanged [67].

Although methods for determining inorganic species via QDs without masking agents have been reported [68], the addition of auxiliary complexing reagents to enable selective determination is very common, especially for inorganic species. Among the most commonly used masking agents is ethylenediaminetetraacetic acid (EDTA). The selective determination of Fe(III) using poly(ethylene glycol)-passivated graphene quantum dots (PEG-GQDs), for example, could be made possible via the use of EDTA. In addition to Fe(III), various ions, such as Cu(II), Co(II), Ni(II), Pb(II) and Mn(II), are responded to by PEG-GQD fluorescence. However, the use of EDTA as a chelating agent to mask these ions allows for selectively determining iron [69]. In another application, the use of CYS-capped QDs for the fluorescence determination of As(III) was only possible after the addition of EDTA as a masking agent, especially because of the interference effect of Cu(II) [70].

Sometimes, masking agents must be combined to obtain a selective determination. The presence of Ag^{+}, Hg^{2+} and Cu^{2+} interferes with the determination of H_2O_2 in human serum upon fluorescence enhancement of CdTe QDs by a hepatitis B core antibody labeled with horseradish peroxidase (HBcAb-HRP). The selective determination of H_2O_2 was only possible using NH_4OH and sodium diethyldithiocarbamate (DDTC) as masking agents. This possibility arose because NH_4OH chelates with Ag^{+} and Hg^{2+}, and DDTC sulfide bonds can capture Cu^{2+}, thereby preventing interference [71].

Sometimes, the combination of multiple strategies can make the procedure even more selective. A change in the crystallite size of the glutathione-capped CdTe QDs (GSH−capped CdTe QDs) in combination with the use of a masking agent proved to be a successful strategy for improving the selectivity. The GSH-capped CdTe QDs with a size of 2.98 nm were more sensitive to Pb(II), whereas those with a size of 3.48 nm were insensitive to Pb(II) and sensitive to Cr(VI). In addition, the interference of other cations by the quenching effect can be solved with EDTA, allowing the application of GSH-capped CdTe QDs as fluorescent probes for Cr(VI) [72]. Nevertheless, for many real samples, the number of concomitant species might be much greater, and simple adjustment of probe dispersion is inefficient.

2.3. Sample preparation

The main limitation of developing QD-based methods is their application in samples with complex matrices, owing to the lack of selectivity observed in some cases. Moreover, the sample matrix can also contain organic and/or inorganic species that can impair the fluorescent properties of QDs, leading to poor-quality results. To overcome these issues caused by matrix concomitants, QD methods combined with various sample preparation strategies have been developed.

For example, several studies seeking to determine inorganic species have performed sample digestion in acidic media. The digestion procedure allows the extraction of the analyte into an aqueous medium, enabling the construction of calibration curves with standards similarly prepared. Furthermore, digestion eliminates potential organic interferences, allowing the application of quantum dots prepared in aqueous media in the analysis of complex solid matrices (*e.g.,* dietary supplements, popcorn, instant noodles, vegetables and soils), oily samples (*e.g.,* biodiesel) or analyte oxidation conversion for total content determination [30,73–79].

Nonetheless, digestion procedures are usually laborious and require the use of strong acids, heat and auxiliary oxidants, such as hydrogen peroxide. Moreover, a procedure for eliminating the reagents used in digestion, which could include neutralization, additional heating, or dilution, must often be employed after digestion. Alternative procedures involving liquid-phase extraction and solid-phase extraction, especially their miniaturized versions, have been used to separate the analyte into a less complex and interference-free phase for later determination via quantum dot-based fluorometric methods.

2.3.1. Extraction of volatile species

Various vapor generation methods have been developed to determine inorganic species via QDs (seeTable 2). In this context, hydride generation (HG) through derivatization with tetrahydroborate (THB) in aqueous media should be highlighted [80]. The generation of hydride is commonly used as a method for sample insertion in spectrometric techniques since the generation of volatile species reduces the matrix effect and increases the sensitivity of the method because the hydride can be generated even from species that are at trace and ultratrace levels [81]. Therefore, the use of HGs has gained prominence in the pretreatment of samples and can be further improved when associated with gas–liquid extraction methods [82]. For example, Butwong and coworkers [83] promoted As speciation by adopting hydride generation associated with a gas–diffusion unit in a stop-flow injection system using a solution of CdS QDs coated with mercaptoacetic acid (MAA-CdS) as the acceptor stream and an analytical probe. With respect to system automatization and analytical performance, under these circumstances, a considerable volume of QD solution was needed, which can be considered a hindrance, especially in comparison with the efficient headspace single-drop microextraction (HS-SDME) approach for volatile species previously demonstrated (Costas-Mora et al., 2011) [84]. In this work, a single drop of QDs was evaluated for the first time, and the authors reported a 500-fold reduction in reagent consumption and considerable luminescence quenching against five volatile species (Fig. 3a). Complementary studies have shown the influence of QD stabilizing agents in nonpolar extractant drops as well as their selectivity and sensitivity improvement (Costas-Mora et al., 2012) [85].

Other procedures without HG derivatization were employed for the QD–HS–SDME extractions. For example, volatile organic compounds were determined in fish samples via an HS-SDME approach in which an ionic liquid/CdSe/ZnS QD drop was used [86]. Owing to the reliance on analyte-promoted QD fluorescence modulation, fluorescence quenching that increased with increasing analyte concentration was observed in most of these systems. In all the studies, the analyte was extracted and preconcentrated directly on a single drop composed of a QD stabilized with nonpolar ligands and dispersed in organic solvents. In this assembly, easy solubilization of the volatile species was observed, even with reduced volumes of QD/solvent dispersion. The great advantage of the QD–HS–SDME system over other strategies that use QDs in aqueous media is the increase in selectivity due to the separation of the target species by volatilization and preconcentration in a single drop.

Nonetheless, HS-SDME systems could be laborious and challenging owing to drop instability. An interesting alternative is the immobilization of QDs into solid supports, which has shown great suitability for HG systems. For example, in an HG-SPE approach, the QDs were immobilized onto a solid support (chromatographic paper), which was attached to a vial cap [87](Fig. 3b). The formed hydride, H_2X (X = As, Bi, Ge, Pb, Sb, Se, Sn, Te, etc.), was extracted and then reacted with the QDs immobilized on the paper support, promoting a decrease in the QD PL that increased with increasing analyte concentration. This phenomenon is easily perceived by the naked eye, allowing visual detection. Using

Table 2
General overview of headspace and liquid extraction approaches for QD-based methods.

Extraction approach	System	QD	Analyte	Potential interferent tested	LOD	LOQ	Ref.
SDME	HS-SDME	HDA-CdSe/ZnS	Se(IV) and CH_3Hg^+	$CaCO_3$, $Fe(NO_3)_3$,KNO_3, and Hg(II)	0.5 μg L^{-1} and 34.5 μg L^{-1} were obtained for Se (IV) and CH_3H^+, respectively	n.a	[97]
SDME	QDs–HS–SDME-μFS	CdSe	Se(IV)	$CaCO_3$, $MgNO_3$, $CaSO_4$, EDTA, Al(III), Cu(II) and humic acid	<0.08 μg L^{-1}	0.4 μg L^{-1}	[85]
SDME	(QD) IL–HS–SDME	CdSe/ZnS	Trimethylamine (TMA)	monomethylamine (MMA), dimethylamine (DMA), propylamine (PA) and diethylamine (DEA)	14 μg L^{-1} (0.35 mg TMA per gram of fish)	47 μg L^{-1} (1.17 mg TMA per gram of fish)	[86]
LLE	HG-FIA-QD	MAA-CdS	As(III) and As(V)	Hg(II)	20 μg L^{-1} for As(III) and 40 μg L^{-1} for As(V)	n.a	[83]
DLLME	UA-TIL-DLLME	CdS	Cu(II)	Cd^{2+}, Zn^{2+} Al^{3+},Co^{2+}, Cr^{3+} Na^+, Li^+, Ni^{2+}, K^+ Ca^{2+}, Mn^{2+}, As^{3+}, CO_3^{2-}, NO_3^-, Cl^-, PO_4^{3-}, SO_4^{2-}, Fe^{3+}, Pb^{2+}, Hg^{2+}	0.28 and 0.026 μg L^{-1} for FL and CL methods, respectively	n.a	[96]
LLLME-CL	LLLME-CdSe-H_2O_2	CdSe–H_2O_2	Sb(III) and Sb	Fe(III), Al(III), Co(II), Cu(II), Ni(II), Se(IV), As(III), $MgCl_2$, EDTA, KNO_3, $CaSO_4$, $CaCO_3$ and humic acid	0.006 μg L^{-1}	0.020 μg L^{-1}	[95]
DLLME	UA-DLLME	GSH-CdTe	Cu(II)	I^-, Br^-, NO_3^-, CO_3^{2-},SO_4^{2-} and PO_4^{3-}, Ca(II), K(I), Mg (II), Al(III), Fe(III), As(II), Co(II), Pb(II), Mo(VI), V (IV), Cr(III), Mn(II), Ni(II), Zn(II) Se(II) and Cu (II)	0.67 μg L^{-1}	2.2 μg L^{-1}	[73]
LLE	LLE-N-GQD	N-GQDs	TiO_2NPs	n.a	1.4 μg g^{-1}	4.67 μg g^{-1}	[92]
DLLME	IL–DLLME-QD	TGA-CdS	Pb(II)	Li^+, Hg^{2+}, Co^{2+}, Cu^{2+}, K^+, CO_3^{2-}	0.004 μg L^{-1}	n. a	[98]
LLME	VA-LLME	F-CDs	4-Nitrophenol	4- chlorophenol (4-CP), 3-chlorophenol (3-CP), 2-chlorophenol (2-CP), phenol, hydroquinone(HQ), 2NP, 3-NP, metal ions Al^{3+},Mg^{2+},Zn^{2+},Cu^{2+},Ba^{2+}, Cd^{2+},Ag^+,Pb^{2+},Ca^{2+}, Mn^{2+},Hg^{2+} and Fe^{3+}	2.1 μg L^{-1}	7 μg L^{-1}	[93]
LLE	Salting-out LLE	N-CDs	Sunitinib	n.a	30 μg L^{-1}	100 μg L^{-1}	[94]

n.a: non-available.

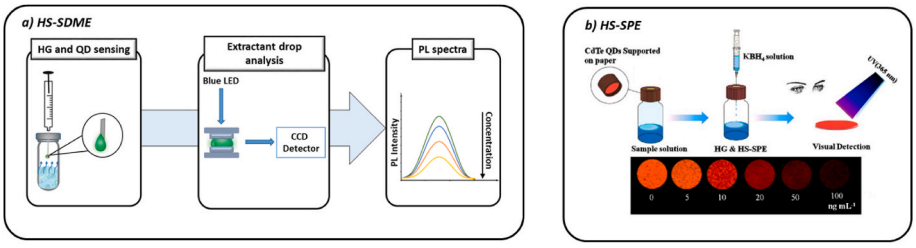

Fig. 3. Headspace extraction manifold using a) single drop and b) solid phase for QD-based methods. Adapted with permission from [87,97]. Copyright 2011 and 2016 ACS Publications, respectively.

this system, Se(IV) [87,88], Zn(II) [89], Ag(I) [90], and As(III) [91] can be detected. Owing to the headspace approach, the separation of analytes from the matrix sample allows the utilization of QD dispersions or solid composites as the acceptor phase and eliminates the need for an elution step before analysis.

2.3.2. *Liquid-phase extraction*

The well-known advantages of extraction procedures associated with analyte separation and preconcentration have been widely exploited for fluorescence methods using QD probes (Table 2). The different possibilities for QD composition and surface modification permitted the preparation of stable probe extraction phase dispersions. Recently, a growing search has been performed to develop miniaturized systems for chemical analysis, which have many distinct advantages, such as rapid analysis and the use of a smaller volume of samples and reagents, leading to a reduction in their consumption and waste generation. For example, the liquid–liquid extraction approach was used to determine titanium oxide nanoparticles (TiO_2NPs) in sunscreens via the use of graphene quantum dots as probes [92]. Vortex-assisted liquid–liquid microextraction (VA-LLME) for the determination of 4-nitrophenol (4-NP) employs nanoprobes of fluorine-doped CDs (F-CD) [93] via organic solvents, such as hexane, methanol and n-octanol. Salting-out liquid–liquid extraction in combination with organic solvent (*e.g.*, acetonitrile) extraction was shown to be an alternative to avoid the effects of the rat blood plasma matrix on nitrogen-doped carbon dots (N–CDs) for sunitinib determination [94]. In both instances, the good dispersibility of CD in organic solvents was crucial for guaranteeing efficient method application. In addition to CDs, binariesl of metallic QDs capped with long-chain organic molecules to improve lipophilicity could be used. However, these lipophilic nanoprobes usually exhibit reduced quantum yields, which impairs method sensitivity.

The liquid–liquid–liquid extraction strategy could be an alternative for employing hydrophilic QDs. Interestingly, Costas-Mora and coworkers reported that Sb, Se and Cu quenched the chemiluminescence of the CdSe–H_2O_2 system. To improve selectivity, a drop liquid–liquid–liquid microextraction (LLLME) method was developed to determine Sb (III) and total Sb. To perform the extraction, diethyldithiocarbamate, a metal chelator, and toluene, a solvent, were used. Nevertheless, in the final extraction step, the metal complex in the organic phase was back-extracted by Triton X-114 aqueous micelles, which led to high selectivity and very low detection limits [95]. Similar LLL approaches could be further exploited to allow the utilization of water-compatible QDs as analytical probes.

In addition to hazardous organic solvents, ionic liquids (ILs) have also been evaluated for the implementation of QD-based fluorescent methods. Water samples were analyzed for Cu^{2+} determination using

ultrasound-assisted dispersive microextraction at a controlled temperature and an ionic liquid as an extraction phase (UA-TIL-DLLME). After the sonication and centrifugation steps, the IL phase was back-extracted with diluted HNO_3 to allow the release of the analyte from the dithizone complex previously formed [96]. Likewise, ionic Pb was extracted from water model samples without mixture sonication. Similarly, in digestion procedures that employ acid reagents, the back-extracted supernatant must be neutralized with NaOH before mixing with the QD–analyte solution.

Aqueous diluted acid/H_2O_2 solutions have also shown good accuracy for ionic metallic determination in biodiesel samples when a glutathione-capped CdTe fluorescent probe was employed. The hydrophilicity of the analyte- and thiol-capped QDs allowed Cu^{2+} extraction and nanocrystal dispersion stability. However, the oxidative medium necessary for analyte conversion and extraction into water demands an additional step for H_2O_2 excess elimination due to possible glutathione oxidation [73].

The results obtained in the aforementioned works confirmed that liquid extraction is an effective tool for analyte isolation and/or sample clean-up. However, solvent toxicity, extractant–QD compatibility and excess reagent usage in eventual additional steps that might be needed, such as analyte derivatization by complexation or oxidation, acid neutralization and reactant decomposition, remain considerable restraints for the more widespread application of these methods.

2.3.3. *Solid-phase extraction*

Solid-phase extraction is another sample preparation approach characterized by reduced consumption and exposure to the solvent, low waste generation, and reduced sample preparation time. This strategy is widely used for analyte isolation and concentration in different sample matrices, as well as a clean-up step to remove possible interferents [99]. Considering QD-based methods, these properties are interesting because the final eluate composition can be controlled. Thus, methods have recently been developed on the basis of the use of cationic exchange columns; nanostructured materials, including magnetic nanoparticles; and molecular recognition sorbents, such as aptamers, immunosorbents, MIPs and IIPs [100,101]. With respect to the QD luminescent methods associated with SPE strategies, a typical approach was to use two different materials for the solid phase and a fluorescent probe. In this case, the analyte was extracted by using a selected solid support, which was followed by a suitable elution step that allowed subsequent analyte probing using QDs as the sensing elements (Fig. 4) (Table 3).

Ionic exchangers have demonstrated good efficiency for inorganic species determination via QD-sensing platforms [102,103]. Inorganic As speciation was performed via the anionic exchanger Amberlite IRA-410 before L-cysteine-capped CdS sensing. Likewise, the selectivity of histamine determination in tuna fish with amino-functionalized graphene quantum dots was ensured by adjusting the sample pH, followed by extraction with the Amberlite CG-50 cationic adsorbent. In both cases, for solid-phase elution, diluted HCl solutions were employed, enabling the pH adjustment of the QD probe with a small solution volume [104,105]. Since multiple charged species can be simultaneously trapped in ionic exchanges, many potential interferents could be present in the eluate solutions. Park and coworkers employed Ambersep GT74 as a solid phase for Pb determination in water samples via graphene oxide quantum dots (GOQDs). This cationic exchanger has a greater affinity for Hg, Ag and Cu than for Pb ions. The selectivity evaluation revealed similar fluorescence variations for the cited species and the analyte when nonmodified GOQDs were applied. However, GOQD surface modification with a DNA aptamer provides adequate analytical performance and is even more effective than SPE in terms of selectivity improvement [106].

In this context, magnetic particles stand out because of their unique properties, such as low organic solvent consumption, easy handling and reduced extraction times. Magnetic solid-phase extraction (MSPE) systems, under optimized conditions, are mostly used to extract and separate analytes from a sample before measurement. After a predetermined contact time, the magnetic material (adsorbent) carrying the analyte is magnetically separated from the solution and subsequently desorbed and analyzed. However, in some cases, MSPE can also be used to bind and remove impurities in a clean-up step, leaving the analyte in the supernatant for direct analysis or further processing. Several studies have reported the use of Fe_3O_4 nanoparticles functionalized with carbon nanomaterials as adsorbents for the extraction and preconcentration of different analytes.

NPs of Fe_3O_4 were used to remove coexisting substances in tobacco samples for the determination of nicotine content, and copper and nitrogen-doped carbon dots (Cu-NCDs) were used as fluorescent probes [107]. The tobacco underwent liquid-assisted ultrasound extraction, but the resulting extracts contained several compounds that could compromise the effectiveness of the QD probe. Consequently, magnetic particles were employed for complementary cleanup of the extractants, leading to improved accuracy (evaluated by recovery tests) and precision. This magnetic purification method was also applied in human serum to remove plasma proteins, peptides, and fats. Fatty acid-coated magnetic nanoparticles (Fe_3O_4@C_6) were synthesized for this purpose, enhancing the physisorption of the matrix constituents via hydrophobic interactions. The MPSE cleanup increased the degree of QD quenching, thereby increasing the sensitivity of the method.

In another work, magnetic nanoparticles (MNPs) were used as analyte adsorbents to determine norfloxacin (NOR) or ciprofloxacin (CIP) in milk samples via the use of sulfur-doped carbon dots (S-CDs) [108]. Once again, the implementation of the MPSE step clearly reduced systematic and aleatory errors. Analyte MSPE adsorption was also applied for ionic copper quantification in wine samples. The core–shell Fe_3O_4@Al_2O_3 NPs were functionalized with polyacrylonitrile (PAN) and dodecyl sulfate to permit Cu^{2+} complexation and extraction. Metal extraction could be carried out without any previous wine treatment,

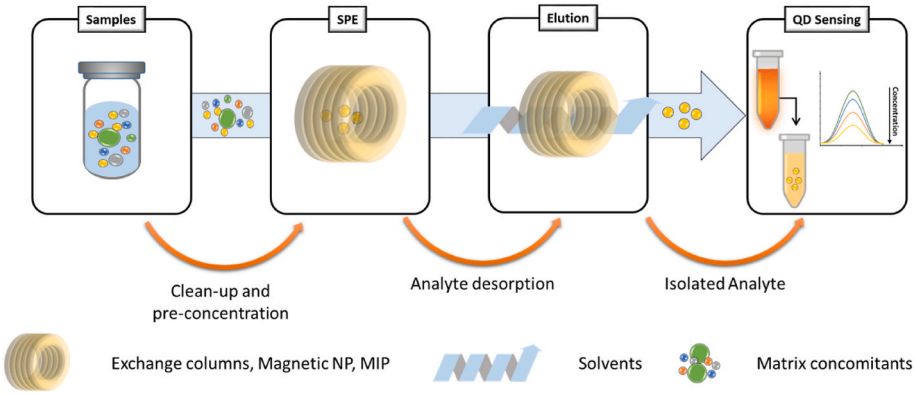

Fig. 4. Schematic representation of the workflow for SPE in QD-based methods.

Table 3
General overview of solid-phase extraction approaches for QD fluorescence methods.

Strategy	System	QD	Analyte	Potential interferent tested	LOD	LOQ	Ref.
SPE	SPE-CYS-CdS (Amberlite IRA-410)	CYS-CdS	As(V)	$Ca2^{+}$, Mg^{2+}, Na^{+}, K^{+}, $NH4^{+}$, Cl^{-}, NO^{3-} $SO4^{2-}$, HCO^{3-}, AsO^{2-}, Co^{2+}, Ni^{2+}, Cu^{2+}, Mn^{2+}, Ni^{2+}, Fe^{2+}, Zn^{2+} Pb^{2+}, Cd^{2+}, Hg^{2+}, I^{-}, $PO4^{3-}$, Ag^{+}, Cr^{3+},Fe^{3+}	0.75 μg L^{-1}	n.a	[105]
MSPE	Fe_3O_4@SiO_2–CdTe-MIPs	CdTe	4-Nonylphenol	BPA, 4-CP and Phe	55087 μg L^{-1}	n.a	[110]
MSPE	Fe_3O_4@CdTe	CdTe	Hydrogen peroxide and glucose	Lactose, fructose, maltose, sucrose, agarose, mannose, xylose, Ca^{2+}, K^{+}. Na^{+}, Mg^{2+}, Zn^{2+}	1190.5 μg L^{-1}, and 72060 μg L^{-1}, respectively	n.a	[111]
SPE	DNA-GOQD	GOQD	Pb(II)	Mn^{2+}, Mg^{2+}, Cd^{2+}, Ca^{2+}, Na^{+},Cu^{2+}, NH_4^{+}, K^{+}, Zn^{2+}, Hg^{2+}, Ag^{+}, Co^{2+}, Ni^{2+}, Fe^{2+}, and Fe^{3+}	0.132 μg L^{-1}	n.a	[106]
SPE	SPE-CdTe (Imobilizaded paper)	CdTe	Se(IV)	Ag^{+},Cu^{2+},Zn^{2+},Fe^{3+}, and Mn^{2+}	0.1 μg L^{-1}	n.a	[87]
SPE	SPE-CdTe (Imobilizaded paper)	CdTe	Ag(I)	Na^{+},K^{+},Pb^{2+},Cu^{2+},Zn^{2+},Ni^{2+},Fe^{3+}, Ca^{2+} and Cr^{3+}	<0.001 μg L^{-1}	n.a	[90]
CPE	CPE-Diglycolamide-CdS/ZnS	Diglycolamide-CdS/ZnS	U(VI)	Li^{+}, Na^{+}, K^{+}, $Mg^{2+}Ca^{2+}$, $Sr2^{+}$, Ba^{2+} Cu^{2+}, Ni^{2+}, Zn^{2+} Co^{2+},Mn^{2+}, Al^{3+}, Fe^{3+}, Cr^{3+}, Cd^{2+}, Pb^{2+}, Hg^{2+}, La^{3+}, Ce^{4+}, Eu^{3+}, SO_4^{2-}, CO_3^{2-}, NO_3^{-}, Cl^{-}, Br^{-}	0.03 μg L^{-1}	n.a	[112]
MSPE	MNP-S-CDs	S-CDs	Norfloxacin and ciprofloxacin	ofloxacin (OFL), difloxacin (DIF), fleroxacin (FLE), pefloxacin (PEF), enoxacin (ENO), levofloxacin (LEV)	1.47 μg L^{-1} and 2.22 μg L^{-1} for NON and CIP, respectively.	n.a	[108]
SPE	HG-SPE-AuNCs (Imobilizaded paper)	BSA–AuNCs	Zn(II)	Fe^{3+}, Hg^{2+}, Cu^{2+}	3 μg L^{-1} and <20 μg L^{-1} for convencional method and visual detection, respectively.	n.a	[89]
MSPE	AuNP/MNP-CdSeS	CdSeS	Norovirus	influenza virus A(H7N7), influenza virus A(H9N2), hepatitis E virus-like particle, and zika virus	0.48 pg mL^{-1}	n.a	[113]
SPE	SPE-GOQD	GOQD	As(III), Cd(II), Pb(II)	Cd^{2+},Cu^{2+},Pb^{2+},Hg^{2+},Ag^{+}, and Fe^{3+}.	0.38 μg L^{-1}, 4.62 μg L^{-1}, and 0.92 μg $L^{-1}$for As^{3+}, Cd^{2+}, and Pb^{2+}, respectively.	n.a	[114]
SPE	HG–HS–AuNCs	AuNCs	Se(IV)	Fe^{3+},Pb^{2+},Sn^{4+},Zn^{2+},Cd^{2+},Sb^{3+},Cr^{3+}, Mn^{2+},Co^{2+},Ni^{2+}, Au^{3+}; Ag^{+},Hg^{2+},Bi^{3+}, As(III), and Cu^{2+}	4 μg L^{-1}	n.a	[88]
MSPE	MCOF-MIPS-CDs	CDs	2,4,6-Trinitrophenol	Ni^{2+}, Mn^{2+}, Ba^{2+}, Pb^{2+}, Zn^{2+}, Mg^{2+}, Ca^{2+}, Co^{2+}, Cd^{2+}, Al^{3+}, Cu^{2+}, Na^{+}, K^{+}, Fe^{2+} and Fe^{3+}	0.22 μg L^{-1}	n.a	[115]
MSPE	Fe_2O_3/TiO_2-MSA-CdTe	MSA-CdSe	Histamine	isoleucine, threonine, proline, phenylalanine, valine, lysine, tryptophan, aspartate, glutamate, and structurally similar histidine were	177.84 μg L^{-1}	6 μM	[116]
MSPE	MHS-CdSeTeS (Fe_2O_3)	CdSeTeS	Hepatitis E virus (HEV), HEV-like particles (HEV-LPs), norovirus-like particles (NoV- LPs), and norovirus (NoV)	hepatitis E virus (HEV), HEV-like particles norovirus-like particles (NoV-LPs), and norovirus (NoV)	0.0000012 μg L^{-1}	n.a	[117]
SPE	SPE-MSA-CdTe (immobilized paper)	MSA-CdTe	As(III)	Na^{+}, K^{+}, NH_4^{+}, CO_3^{2-}, SO_4^{2-}, and S^{2-}, Hg^{2+},Pb^{2+}, and Sn^{2+}	0.000016 μg L^{-1}	0.053 mg L^{-1}	[91]
MSPE	Fe_3O_4–Cu-NCDs	Cu-NCDs	Nicotine	Ca^{2+}, Mg^{2+}, Mn^{2+}, Ni^{2+}, Pb^{2+}, Co^{2+}, Fe^{3+}, Fe^{2+}, Zn^{2+}, Al^{3+}, glucose, maltose, sucrose, glycine (Gly), cysteine (Cys), methionine (Met) and glutamic (Glu), oxalate, citric acid, succinic acid, malic acid, gallic acid, catechol, phloroglucinol and phenol	0.00001 μg L^{-1}	n.a	[107].

n.a: non-available.

suggesting great selectivity [109]. Furthermore, the elution step was performed using the carbon dot dispersion itself, resulting in a very easy operating method. Truly challenging samples, such as biological fluids and beverages, can be analyzed with accuracy and precision via effortless procedures facilitated by various modified MPs. Another relevant aspect was the need for only small volumes of eluent, although organic solvents are still necessary, especially for organic analytes. From this viewpoint, the stability of QD dispersions remains a concern. Despite the great achievements in selectivity resulting from MPs and their modifications, simultaneous extraction of potential interferents for NP methods could occur. Recently, chemometric tools have emerged as powerful alternatives to improve fluorometric data analysis, even for complex sample matrices.

2.4. Chemometric analysis in QD-based methodologies

As previously described, distinct analytical strategies have been implemented to overcome QD selectivity issues that could impair the detection of single analytes in complex sample matrices or the determination of multiple analytes in the same analysis [118].

Unfortunately, most of these works adopt a classical analytical calibration relying on the measurement of a single signal per sample. This easily available and simple type of data is conveniently applied in analytical chemistry, but the running analytical approaches require total

selectivity toward the analyte of interest. To obtain this total selectivity, complex operations have been implemented, as described in the previous subsections of the manuscript.

An interesting and expeditious alternative relies on multivariate calibration methods, which require more data to be acquired per sample but provide much more information about the QD–analyte interaction process. Because it is more complex, the acquired data cannot be handled by a linear regression model and must be processed by more elaborate multivariate algorithms [119]. Distinct chemometric models have been used to analyze the PL dataset (see Table 4), allowing useful information on QD-based sensing events to be obtained. The application of statistical and mathematical methods helps identify the interconnection between the evaluated variables, improving the figures of merit of the developed methodologies and acting as an effective strategy to increase selectivity. The selection of the most appropriate chemometric model depends on several factors, such as 1) the purpose of the analysis (to discriminate, identify or quantify); 2) the complexity (first, second or higher-order data) and the properties (such as the trilinearity or its absence) of the obtained data; and 3) the relationship between the analyte concentration and the PL data, which could be linear or nonlinear [120]. Occasionally, even after using all of the above-described strategies, some compounds may still interfere with the determination of the analytes. In these cases, only chemometric methods based on multivariate calibration are prone to circumvent the occurrence of this interfering species.

To successfully implement QD-based PL methodologies for analytical purposes, it is important to consider the kind of sample (matrix complexity) under analysis and, consequently, what type of data will be required to obtain an accurate and selective determination of the analyte. The data obtained via QD-based PL methods are classified according to their complexity and can be considered zeroth-, first-, second-, and higher-order data. The amount of acquired data and the most suitable chemometric model are subsequently chosen considering the complexity of the sample matrix. When the QD–analyte interaction process is evaluated by measuring the fluorescence intensity at a single maximum emission wavelength, zero-order data, which are mostly used in univariate calibration methods, are obtained. Their use is only recommended if total selectivity for the analyte is guaranteed. In these cases, the presence of an interfering species that impairs the ability of the analyte to respond to the PL signal cannot be compensated for. Unlike univariate calibration, multivariate methods allow circumventing the presence of nonanalytes in a sample. When multivariate calibration methods are used, the acquisition of more complex data arrays per sample, such as first-, second-, and higher-order data, is more suitable, as it allows the performance of quantitative and/or qualitative determination with enhanced selectivity. First-order data are obtained when an emission spectrum is recorded for the QD–analyte interaction process at each analyte concentration, which corresponds to vector data for a single sample. The analysis of this type of data enables the first-order advantage to be obtained. This benefit means that the selective and accurate quantification of the analyte in samples with interfering species is possible when these interferents are included in the calibration process. The first-order advantage is only useful for determining analytes in samples with known constituents, such as pharmaceutical formulations, dietary supplements, and some food samples with labeled contents. Therefore, in this case, the presence of unexpected constituents in the samples can impair analyte determination [121].

Several QD-sensing schemes have been proposed to explore the chemometric analysis of the obtained first-order data. A common strategy that could be used to improve the selectivity of the analysis is the combination of multiple fluorescent nanoparticles in a single emitter nanoprobe. The use of multiple-emitter nanoprobes composed of multiple QDs of different sizes, configurations, natures, and/or compositions or the combination of QDs with other fluorescent probes and/or nanomaterials can enhance the quality of the acquired information. Therefore, by using a multiemitter combined nanoprobe, the PL response is based on simultaneous analyte-induced modulation of the PL intensities of more than one emission band at distinct wavelengths, which results in a specific analyte–response profile with multipoint detection.

A work that illustrates the importance of the use of a multiemitter nanoprobe is the combination of two distinctly sized MPA-capped CdTe QDs as a fluorometric probe for the detection and differentiation of distinct divalent metals, namely, copper, lead, and mercury [122]. Each metal ion caused a distinctive response on the PL nanohybrid probe, making its quantification in a binary or ternary mixture possible. Principal component analysis (PCA) and partial least squares (PLS) were used for fluorescence data analysis. Concerning the binary mixture, the obtained results indicated that a concentration estimation of each metal ion was possible since the values of the coefficient of determination of cross-validation (R_2CV) were satisfactory. Nevertheless, when the three

Table 4
QD-based PL methodologies use chemometric models to circumvent selectivity issues.

Data structure	Sensing platform	Analyte	Chemometric model	Potential interferent tested	LOD	LOQ	Ref.
Two-way	MPA-CdTe/MPA-CdTe	Hg^{2+} Cu^{2+} Pb^{2+}	PCA, PLS	n.a	n.a.	n.a	[122]
Two-way	GSH-CdTe/MPA-CdTe MPA-CdTe/MPA-CdTe	Hg^{2+} Cu^{2+}	PLS	n.a	n.a.	n.a	[123]
Two-way	CYS-CdTe/MPA-$AgInS_2$	Folic acid Fe^{2+}	ANN	n.a	838.7 μg L^{-1} 228.9 μg L^{-1}	2560 μg L^{-1} 681.3 μgL^{-1}	[124]
Two-way	CDs/CYS-CdTe	4-Nitrophenol TNT	ANN	n.a	186.4 μg L^{-1} 717.7 μg L^{-1}	n.a	[125]
Three-way	CYS-CdS	Cu^{2+}	PLS	n.a	0.826 μg L^{-1}	n.a	[126]
Three-way	TMA-$AgInS_2$	OTC	U-PLS	lactose	64 μg L^{-1}	191.6 μg L^{-1}	[127]
Three-way	MPA-CdTe	pH	PARAFAC2, MCR-ALS	n.a	n.a.	n.a	[128]
Three-way	Sulfur QDs	Cu^{2+}, Pb^{2+}, Ni^{2+}, Fe^{3+}, Co^{2+}, Hg^{2+}, Au^{3+}, and Fe^{2+}	LDA, HCA	n.a	n.a.	n.a	[130]

n.a: non-available.

divalent metals were tested simultaneously, Pb^{2+} and Hg^{2+} could be quantified, whereas Cu^{2+} could only be detected, suggesting the occurrence of copper ions but making their quantification unfeasible. One way to circumvent this issue, by allowing accurate discrimination and quantification of multiple analytes present in a complex sample matrix, is the combination of QDs passivated with thiol-based capping ligands with different terminal functional groups, which could confer more distinct responses toward a particular analyte. Alternatively, the addition of a fluorometric probe to a third PL nanomaterial or a conventional organic fluorophore, which emits at a complementary wavelength, could be explored.

In another work [123], CdTe QDs passivated with distinct thiol-based molecules, and consequently with distinctive functional moieties, were arranged into multi-QD nanoplatforms for testing via Hg^{2+} and Cu^{2+} determination. As expected, each multi-QD nanoplatform exhibited a specific fluorometric response for each metal ion, and the respective PL data were analyzed via the PLS model. Therefore, the sensitivity of the developed models was determined to ascertain which combined nanoprobe allowed a more sensitive determination of Cu^{2+} and Hg^{2+}. For mercury quantification, the sensitivity of the GSH/MPA combined nanoplatform was approximately 7 times greater than that of the 3-morpholinoethanesulfonic (MES)/MPA conjugated probe (Fig. 5a), whereas for copper quantification, the MPA/MPA combined probe showed greater sensitivity (Fig. 5b). Both works demonstrated the advantage of using combined nanoprobes with subsequent chemometric analysis of the acquired first-order data (emission spectra) to quantify mutually interfering metal ions.

Two other works were developed to simultaneously determine analytes that usually coexist in the same sample, where the determination of each analyte can interfere with the determination of the other analyte because both analytes interact with QDs. The co-occurrence of folic acid and Fe^{2+} in pharmaceutical formulations is popular. Thus, QDs with distinct compositions (Cd-based and Cd-free QDs), namely, L-cysteine (CYS)-capped CdTe and MPA-capped $AgInS_2$ (AIS) QDs, were combined in a dual-emission nanoprobe [124]. Owing to the different reactivities, a specific response profile for each analyte was obtained, which made accurate determination of the two mutually interfering analytes in the same analysis possible upon the use of a suitable chemometric model. Likewise, QDs of different natures (carbon dots or semiconductor QDs), specifically CYS-CdTe QDs and CDs, were used to simultaneously detect 4-nitrophenol (4-NP) and 2,4,6-trinitrotoluene (TNT) [125]. Owing to the nonlinear relationship between the PL data and the analyte concentration, the artificial neural network (ANN) model was revealed to be the most efficient chemometric model for the determination of analytical targets in both works [124,125].

Despite the pertinence of exploring first-order advantages for the determination of the analyte in samples with interfering species that are expected, their use becomes impractical when the samples have a complex matrix in which their contents are unknown. Effectively, in the case of environmental, biological, or food samples, it is not possible to anticipate which interfering species could interfere with the obtained PL signal. An ingenious way to solve this problem is the acquisition of second- and higher-order data of the QD-analyte sensing event, which, upon analysis by suitable chemometric models, allows us to obtain a second-order advantage. In this way, the selective and accurate determination of the analyte becomes possible even in the presence of unknown interfering constituents that were not included in the calibration set [121].

The second-order data correspond to obtaining a matrix for a single sample, whereas the three-way data correspond to a stack of matrices for all standards or samples in the calibration set. This type of data can be acquired in three different ways: i) the recording of the emission spectra throughout the QD–analyte interaction event, thus evaluating its kinetic process; ii) the acquisition of an excitation–emission (EEM) matrix, which is generated by recording consecutive emission spectra at different excitation wavelengths; and iii) the combination of different

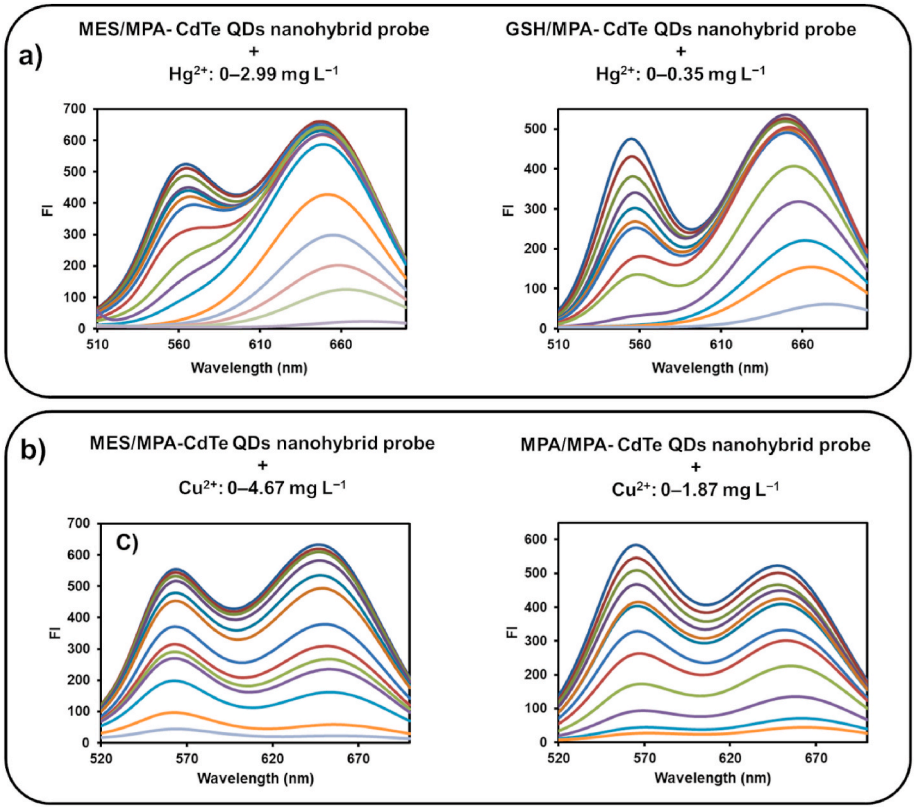

Fig. 5. PL spectra of different combined nanoprobes in the presence of a) Hg^{2+} and b) Cu^{2+} at increasing concentrations. Adapted with permission from [123]. Copyright 2018 Elsevier.

techniques, combining the information provided by diverse sources of the same sample.

An illustrative example of the first described method for obtaining second-order data is the determination of Cu^{2+} via the kinetic fluorescence behavior of CYS-capped CdS QDs in the presence of a metal ion [126]. Additionally, other metal ions were tested (namely, Ag^{+}, Ni^{2+} and Hg^{2+}) and showed characteristic kinetic behavior, which can provide a specific analyte response (metal ion fingerprinting profile) for each metal ion. In the presence of copper ions, the CdS QD PL was gradually inhibited, and a redshift in the emission spectra was observed. The different metal ions caused distinct kinetic behavior in the PL quenching of the CdS QDs, thus allowing the selective and accurate monitoring of Cu^{2+} in the presence of interfering species and making the simultaneous determination of the coexisting metal ions in the same sample possible.

In another methodology [127], the kinetic behavior of $AgInS_2$ QDs in the presence of oxytetracycline (OTC) (quenching induced by OTC) was explored for its selective determination. Initially, a ratiometric sensing approach was developed for OTC determination, which involved a mixture of the antibiotic (used simultaneously as the analyte and dynamic fluorophore) and TMA–$AgInS_2$ QDs. However, the presence of an excipient in pharmaceutical formulations for veterinary purposes has hindered ratiometric measurements. To circumvent the selectivity issues, a kinetic approach was implemented, which not only improved the sensitivity and selectivity but also reduced the LOD. The kinetic PL data were analyzed with unfolded partial least squares (U-PLS), which enabled the quantification of OTC even in the presence of uncalibrated interfering species (Fig. 6a).

Another way to obtain three-dimensional data is the acquisition of excitation–emission matrix (EEM) fluorescence spectra, which encompasses the acquisition of successive PL spectra at consecutive excitation wavelengths. This type of data is difficult to implement mainly because it requires expensive instrumentation, which should allow a three-dimensional spectrum to be obtained as quickly as possible. An illustrative example is the use of MPA-Cd-based QDs to detect pH changes. Modification of the solution pH caused changes in the QD PL intensity as well as deviations in the maximum emission wavelength (redshift) (Fig. 6b). The effects of pH-induced modifications on the optical properties of the QDs were analyzed via multivariate curve resolution alternating least squares (MCR-ALS), which enables the efficient evaluation of the pH effect via second-order data analysis. The analysis of this type of data with proper chemometric tools could allow the application of this QD-based sensing platform in complex samples, such as in biological samples as bioimaging sensors [128].

Unfortunately, EEM data acquisition requires an expensive fluorimeter that can rapidly obtain the PL spectrum at multiple excitation wavelengths. An alternative scheme to obtain more complex data by resorting to simpler instruments is the combination of data from the same sample via multiple sources [129]. *Sun* et al. developed an analytical methodology using sulfur QDs for the qualitative and quantitative analysis of eight metal ions (Cu^{2+}, Pb^{2+}, Ni^{2+}, Fe^{3+}, Co^{2+}, Hg^{2+}, Au^{3+}, and Fe^{2+}). In this work, multiple optical properties (fluorescence,

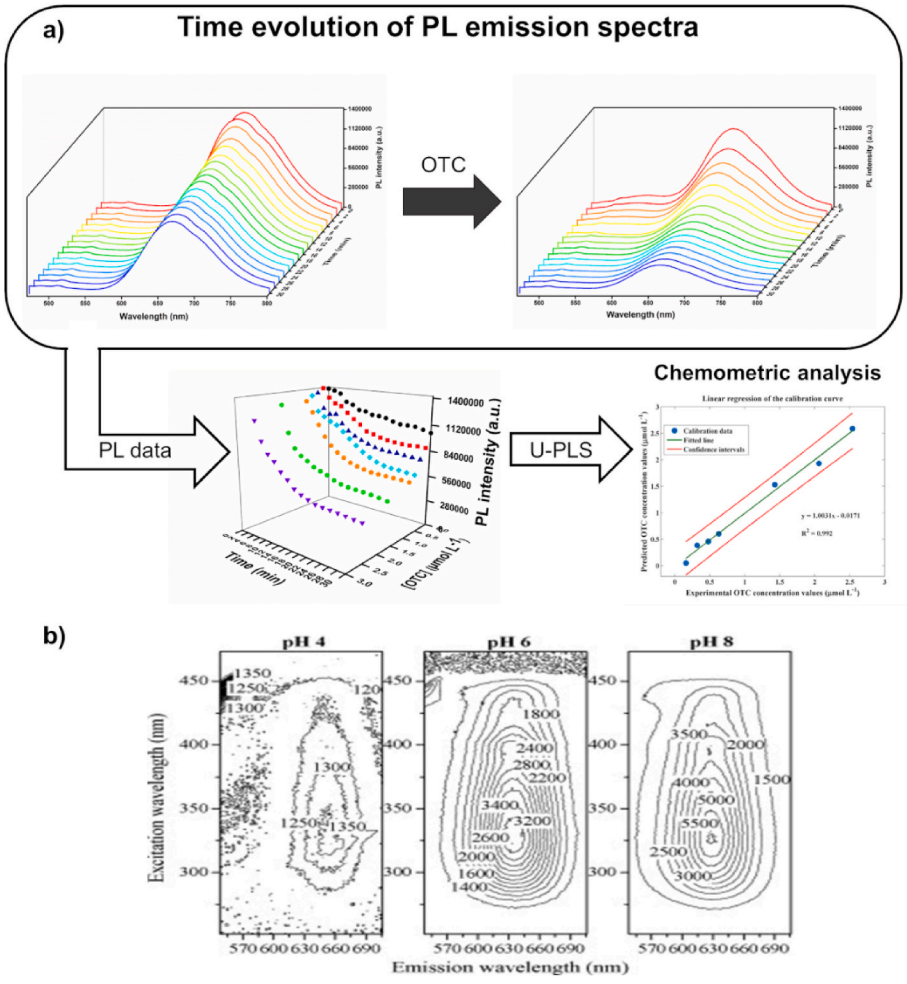

Fig. 6. Different types of three-way data: a) PL spectra during a period of time (three-dimensional data) and the correspondent analysis using the adequate chemometric model. Adapted with permission from [127]. Copyright 2021 Elsevier.; b) second-order EEM data acquired per sample at distinct pH. Adapted with permission from [128]. Copyright 2008 Elsevier.

second-order scattering, and ultraviolet–visible absorption) were used to increase the complexity of the obtained data and, consequently, the efficiency of the sensing platform [130]. The obtained data were analyzed via linear discriminant analysis (LDA) and hierarchical cluster analysis (HCA). As expected, the greater the complexity of the obtained data is, the greater the qualitative discrimination of each metal ion and the semiquantitative analysis of the metal ions in the water samples.

In conclusion, the use of chemometric models in QD-based approaches could circumvent selectivity issues in which the type of acquired data plays an important role. Indeed, multivariate methods can compensate for the occurrence of unknown and uncalibrated species, provided that the obtained data are the most suitable. In fact, selective determinations can be performed without the specific surface functionalization of the sensing elements.

3. Conclusions and future perspectives

The versatility of QDs for sensing different chemical species has been demonstrated in recent decades. However, their claimed multisensing ability often leads to a lack of selectivity, limiting their use in analyzing more complex samples. The basic strategy for improving selectivity has been based on QD surface engineering, along with controlling the probe composition and ideal working conditions (pH, ionic strength, masking agents, etc.). Notably, molecular or ionic imprinted polymer IP@QD composites have emerged as efficient surface-modified materials because of their inherent selectivity. Nevertheless, structural and charge alterations induced by the sample matrix remain challenging. In this sense, extraction methodologies need further exploration to achieve long-term consolidation of QD-based methods and diminish hindrances associated with solvent toxicity, QD solubility, and analyte/matrix segregation. Headspace approaches are effective for segregation and QD dispersion on different extractor phases but remain restricted to volatile species or hydrides. Additionally, the ability of chemometric models to correct unknown and uncalibrated species may complement extraction approaches by reducing interference effects.

Future perspectives in this scenario should focus on expanding analyte derivatization/segregation approaches, as well as unexplored combinations of strategies. For example, UV photochemical vapor generation could offer an alternative to extend headspace extraction methodologies for QD methods. Similarly, ionic liquids and deep eutectic solvents, known for their high tunability and reduced toxicity, require further exploration for the sample preparation steps of QD-based PL methods. Moreover, the extraction kinetic profile could be evaluated to generate a still nonstudied second-order data matrix on the basis of an analyte extraction–fingerprinting profile. These approaches open new alternatives for the application of chemometric tools. Artificial intelligence protocols, such as machine learning, are a remarkable tool for the recognition of patterns and correlations, which could be useful for connections between input fingerprints and output characteristics to predict QD–analyte interactions.

In summary, QD nanoparticles remain promising materials for developing sensitive methods. However, efforts to improve sample preparation procedures and the use of proper chemometric tools will be essential for broadening their application in the coming decades.

Funding

This work received financial support from FCT/MCTES (UIDB/50006/2020 DOI: 10.54499/UIDB/50006/2020) through national funds.

CRediT authorship contribution statement

Rodolfo M.M. Santana: Writing – review & editing, Writing – original draft, Supervision, Conceptualization. **Leila S.V. Barbosa:** Writing – review & editing, Writing – original draft. **Leandro G. Benzi:** Writing – original draft. **Rafael C. Castro:** Writing – review & editing, Writing – original draft. **David S.M. Ribeiro:** Writing – review & editing, Writing – original draft. **Maria Graças A. Korn:** Writing – review & editing, Supervision, Funding acquisition. **João L.M. Santos:** Writing – review & editing, Writing – original draft, Supervision, Funding acquisition, Conceptualization. **Leonardo S.G. Teixeira:** Writing – review & editing, Writing – original draft, Supervision, Funding acquisition, Conceptualization.

Declaration of competing interest

The authors declare that they have no known competing financial interests or personal relationships that could have appeared to influence the work reported in this paper.

Data availability

No data was used for the research described in the article.

Acknowledgments

The authors are grateful to Fundação de Amparo a Pesquisa do Estado da Bahia (FAPESB), Conselho Nacional de Desenvolvimento Científico e Tecnológico (CNPq) and Coordenação de Aperfeiçoamento de Pessoal de Nível Superior (CAPES) for providing grants, fellowships and financial support. All the authors are grateful for support from the Brazil (FAPESB)–Portugal (FCT) bilateral scientific cooperation project. This work received support and help from FCT/MCTES (LA/P/0008/2020 DOI 10.54499/LA/P/0008/2020, UIDP/50006/2020 DOI 10.54499/UIDP/50006/2020 and UIDB/50006/2020 DOI 10.54499/UIDB/50006/2020) through national funds. Rafael C. Castro thanks FCT (Fundação para a Ciência e Tecnologia) and POPH (Programa Operacional Potencial Humano) for the Ph.D. grant 2020.08465.BD. David S. M. Ribeiro thanks FCT for funding through the program DL 57/2016 – Norma Transitória (DL 57/2016/CP1346/CT0033, DOI 10.54499/DL57/2016/CP1346/CT0033).

References

[1] Z. Yu, H. Gong, Y. Li, J. Xu, J. Zhang, Y. Zeng, X. Liu, D. Tang, Chemiluminescence-derived self-powered photoelectrochemical immunoassay for detecting a low-abundance disease-related protein, Anal. Chem. 93 (2021) 13389–13397, https://doi.org/10.1021/acs.analchem.1c03344.

[2] Z. Yin, L. Zhu, Z. Lv, M. Li, D. Tang, Persistent luminescence nanorods-based autofluorescence-free biosensor for prostate-specific antigen detection, Talanta 233 (2021) 122563, https://doi.org/10.1016/j.talanta.2021.122563.

[3] Z. Qiu, J. Shu, D. Tang, Bioresponsive release system for visual fluorescence detection of carcinoembryonic antigen from mesoporous silica nanocontainers mediated optical color on quantum dot-enzyme-impregnated paper, Anal. Chem. 89 (2017) 5152–5160, https://doi.org/10.1021/acs.analchem.7b00989.

[4] S. Lv, Y. Tang, K. Zhang, D. Tang, Wet NH_3-triggered NH_2-MIL-125(Ti) structural switch for visible fluorescence immunoassay impregnated on paper, Anal. Chem. 90 (2018) 14121–14125, https://doi.org/10.1021/acs.analchem.8b04981.

[5] L. Manna, The bright and enlightening science of quantum dots, Nano Lett. 23 (2023) 9673–9676, https://doi.org/10.1021/acs.nanolett.3c03904.

[6] Z. Qiu, J. Shu, Y. He, Z. Lin, K. Zhang, S. Lv, D. Tang, CdTe/CdSe quantum dot-based fluorescent aptasensor with hemin/G-quadruplex DNzyme for sensitive detection of lysozyme using rolling circle amplification and strand hybridization, Biosens. Bioelectron. 87 (2017) 18–24, https://doi.org/10.1016/j.bios.2016.08.003.

[7] Z. Lin, S. Lv, K. Zhang, D. Tang, Optical transformation of a CdTe quantum dot-based paper sensor for a visual fluorescence immunoassay induced by dissolved silver ions, J. Mater. Chem. B 5 (2017) 826–833, https://doi.org/10.1039/c6tb03042d.

[8] A.M.C. Jaison, D. Vasudevan, K. Ponmudi, A. George, A. Varghese, One pot hydrothermal synthesis and application of bright-yellow-emissive carbon quantum dots in Hg^{2+} detection, J. Fluoresc. 33 (2023) 2281–2294, https://doi.org/10.1007/s10895-023-03233-z.

[9] H. Zhou, H. Wang, X. Li, L. Wang, H. Huang, H. Qiu, W. Cong, M. Wang, J. Zhang, Synthesis of group I-III-VI semiconductor quantum dots and its application in food safety testing, Rev. Anal. Chem. 41 (2022) 324–336, https://doi.org/10.1515/revac-2022-0054.

[10] C. Yao, J. Qian, F. Chen, Y. Wang, J. Lin, J. Chen, J. Wei, Z. Yang, Design of highly defective Zn-doped CeO_2 solid solution quantum dots for accurate monitoring of

ciprofloxacin, Microchem. J. 193 (2023) 109086, https://doi.org/10.1016/j.microc.2023.109086.
[11] Y. Sheng, Z. Huang, Y. Chen, X. Guo, C. Lan, H. Peng, W. Chen, Facile high-quantum-yield sulfur-quantum-dot-based, Anal. Bioanal. Chem. 414 (2022) 7675–7681.
[12] H. Wu, J.H. Li, W.C. Yang, T. Wen, J. He, Y.Y. Gao, G.F. Hao, W.C. Yang, Nonmetal-doped quantum dot-based fluorescence sensing facilitates the monitoring of environmental contaminants, Trends Environ. Anal. Chem. 40 (2023) e00218, https://doi.org/10.1016/j.teac.2023.e00218.
[13] J. Wu, J. Li, L. Li, W.F. Dong, C. Jiang, F. Zhang, Water-soluble near-infrared CuInS2/ZnS fluorescent quantum dots for Cu2+ detection and cellular imaging, Microchem. J. 199 (2024), https://doi.org/10.1016/j.microc.2024.109962.
[14] S. Ganguly, S. Margel, Fluorescent quantum dots-based hydrogels: synthesis, fabrication and multimodal biosensing, Talanta Open 8 (2023) 100243, https://doi.org/10.1016/j.talo.2023.100243.
[15] I. Costas-Mora, V. Romero, I. Lavilla, C. Bendicho, An overview of recent advances in the application of quantum dots as luminescent probes to inorganic-trace analysis, TrAC, Trends Anal. Chem. 57 (2014) 64–72, https://doi.org/10.1016/j.trac.2014.02.004.
[16] J. Khan, Optical chemosensors synthesis and appplication for trace level metal ions detection in aqueous media : a review, J. Fluoresc. (2024), https://doi.org/10.1007/s10895-023-03559-8.
[17] Y. Lou, J. Zhu, Ultrasensitive optical detection of anions by quantum dots, NANOSCALE HORIZONS (2016) 125–134, https://doi.org/10.1039/c5nh00039d.
[18] S.A. Nsibande, P.B.C. Forbes, Fluorescence detection of pesticides using quantum dot materials – a review, Anal. Chim. Acta 945 (2016) 9–22, https://doi.org/10.1016/j.aca.2016.10.002.
[19] J.V. Kumar, J.-W. Rhim, Fluorescent carbon quantum dots for food contaminants detection applications, J. Environ. Chem. Eng. 12 (2024) 111999, https://doi.org/10.1016/j.jece.2024.111999.
[20] I.Y. Goryacheva, E.S. Speranskaya, V.V. Goftman, D. Tang, S. De Saeger, Synthesis and bioanalytical applications of nanostructures multiloaded with quantum dots, TrAC, Trends Anal. Chem. 66 (2015) 53–62, https://doi.org/10.1016/j.trac.2014.11.008.
[21] E. Yang, Y. Zhang, Y. Shen, Quantum dots for electrochemiluminescence bioanalysis - a review, Anal. Chim. Acta 1209 (2022) 339140, https://doi.org/10.1016/j.aca.2021.339140.
[22] L. Wang, L. Wen, L. Zhao, J. Chao, F. Tao, F. Wang, C. Li, Development of fluorescence sensor and test paper based on molecularly imprinted carbon quantum dots for spiked detection of domoic acid in shellfish and lake water, Anal. Chim. Acta 1197 (2022) 339515, https://doi.org/10.1016/j.aca.2022.339515.
[23] M.H. Abo Zaid, N. El-Enany, A.E. Mostafa, G.M. Hadad, F. Belal, Estimation of two diuretics using fluorescent nitrogen doped carbon quantum dots: application to spiked human plasma and tablets, J. Fluoresc. 33 (2023) 2209–2218, https://doi.org/10.1007/s10895-023-03217-z.
[24] L.S.V. Barbosa, L.S.G. Teixeira, M.G.A. Korn, R.M.M. Santana, Evaluation of the direct interaction between amino acids and glutathione-coated CdTe quantum dots and application in urinalysis for histidine determination, J. Braz. Chem. Soc. 32 (2021) 588–598, https://doi.org/10.21577/0103-5053.20200212.
[25] Q. Zhou, Y. Lin, M. Xu, Z. Gao, H. Yang, D. Tang, Facile synthesis of enhanced fluorescent gold-silver bimetallic nanocluster and its application for highly sensitive detection of inorganic pyrophosphatase activity, Anal. Chem. 88 (2016) 8886–8892, https://doi.org/10.1021/acs.analchem.6b02543.
[26] Y. Lin, Q. Zhou, D. Tang, R. Niessner, H. Yang, D. Knopp, Silver nanolabels-assisted ion-exchange reaction with CdTe quantum dots mediated exciton trapping for signal-on photoelectrochemical immunoassay of mycotoxins, Anal. Chem. 88 (2016) 7858–7866, https://doi.org/10.1021/acs.analchem.6b02124.
[27] K. Zhang, S. Lv, Z. Lin, D. Tang, CdS:Mn quantum dot-functionalized g-C_3N_4 nanohybrids as signal-generation tags for photoelectrochemical immunoassay of prostate specific antigen coupling DNAzyme concatamer with enzymatic biocatalytic precipitation, Biosens. Bioelectron. 95 (2017) 34–40, https://doi.org/10.1016/j.bios.2017.04.005.
[28] J. Shu, D. Tang, Current advances in quantum-dots-base photoelectrochemical immunoassays, Chem. Asian J. 12 (2017) 2780–2789.
[29] M. Alizadeh-Ghodsi, M. Pourhassan-Moghaddam, A. Zavari-Nematabad, B. Walker, N. Annabi, A. Akbarzadeh, State-of-the-Art and trends in synthesis, properties, and application of quantum dots-based nanomaterials, Part. Part. Syst. Charact. 36 (2019) 1800302.
[30] S.S.M. Rodrigues, A.S. Lima, L.S.G. Teixeira, M.D.G.A. Korn, J.L.M. Santos, Determination of iron in biodiesel based on fluorescence quenching of CdTe quantum dots, Fuel 117 (2014) 520–527, https://doi.org/10.1016/j.fuel.2013.09.045.
[31] D.A. Hines, P.V. Kamat, Recent advances in quantum dot surface chemistry, ACS Appl. Mater. Interfaces 6 (2014) 3041–3057, https://doi.org/10.1021/am405196u.
[32] J. Zhu, Z.J. Zhao, J.J. Li, J.W. Zhao, CdTe quantum dot-based fluorescent probes for selective detection of Hg (II): the effect of particle size, Spectrochim. Acta Part A Mol. Biomol. Spectrosc. 177 (2017) 140–146, https://doi.org/10.1016/j.saa.2017.01.043.
[33] M. Li, Y. Ge, Q. Chen, S. Xu, N. Wang, X. Zhang, Hydrothermal synthesis of highly luminescent CdTe quantum dots by adjusting precursors' concentration and their conjunction with BSA as biological fluorescent probes, Talanta 72 (2007) 89–94, https://doi.org/10.1016/j.talanta.2006.09.028.
[34] M. Hua, S. Yang, J. Ma, W. He, L. Kuang, D. Hua, Highly selective and sensitive determination of uranyl ion by the probe of CdTe quantum dot with a specific size, Talanta 190 (2018) 278–283, https://doi.org/10.1016/j.talanta.2018.08.012.
[35] S. Banerjee, S. Kar, S. Santra, A Simple Strategy for Quantum Dot Assisted Selective Detection of Cadmium Ions W, vol. 1, 2008, pp. 3037–3039, https://doi.org/10.1039/b803166e.
[36] M. Green, The Nature of Quantum Dot Capping Ligands, 2010, pp. 5797–5809, https://doi.org/10.1039/c0jm00007h.
[37] S. Silvi, A. Credi, Luminescent sensors based on quantum dot–molecule conjugates, Chem. Soc. Rev. (2015) 4275–4289, https://doi.org/10.1039/c4cs00400k.
[38] Y. Chen, Z. Rosenzweig, Luminescent CdS quantum dots as selective ion probes, Anal. Chem. 74 (2002) 5132–5138, https://doi.org/10.1021/ac0258251.
[39] F. Faridbod, A. Jamali, M.R. Ganjali, A Novel Cobalt-Sensitive Fluorescent Chemosensor Based on Ligand Capped CdS Quantum Dots, 2015, pp. 613–619, https://doi.org/10.1007/s10895-015-1544-y.
[40] A. Zhao, C. Zhao, M. Li, J. Ren, X. Qu, Ionic liquids as precursors for highly luminescent, surface-different nitrogen-doped carbon dots used for label-free detection of Cu2+/Fe3+ and cell imaging, Anal. Chim. Acta 809 (2014) 128–133, https://doi.org/10.1016/j.aca.2013.10.046.
[41] M.P. Shirani, B. Rezaei, A.A. Ensafi, M. Ramezani, Development of an eco-friendly fluorescence nanosensor based on molecularly imprinted polymer on silica-carbon quantum dot for the rapid indoxacarb detection, Food Chem. 339 (2021) 127920, https://doi.org/10.1016/j.foodchem.2020.127920.
[42] H. Liu, L. Ding, L. Chen, Y. Chen, T. Zhou, H. Li, Y. Xu, L. Zhao, N. Huang, A facile, green synthesis of biomass carbon dots coupled with molecularly imprinted polymers for highly selective detection of oxytetracycline, J. Ind. Eng. Chem. 69 (2019) 455–463, https://doi.org/10.1016/j.jiec.2018.10.007.
[43] W. Zhang, S. Ye, Y. Diao, X. Deng, W. Li, H. He, Q. Liu, G. Hu, Magnetic multi-walled carbon nanotubes modified with surface-imprinted polymers for ultrasensitive electrochemical detection of trace-level nickel ions in groundwater, Mater. Today Chem. 35 (2024) 101863, https://doi.org/10.1016/j.mtchem.2023.101863.
[44] E.Y. Bivián-Castro, A. Zepeda-Navarro, J.L. Guzmán-Mar, M. Flores-Alamo, B. Mata-Ortega, Ion-imprinted polymer structurally preorganized using a phenanthroline-divinylbenzoate complex with the Cu(II) ion as template and some adsorption results, Polymers 15 (2023), https://doi.org/10.3390/polym15051186.
[45] X. Luo, B. Guo, L. Wang, F. Deng, R. Qi, S. Luo, C. Au, Synthesis of magnetic ion-imprinted fluorescent CdTe quantum dots by chemical etching and their visualization application for selective removal of Cd(II) from water, Colloids Surfaces A Physicochem. Eng. Asp. 462 (2014) 186–193, https://doi.org/10.1016/j.colsurfa.2014.09.012.
[46] Z. Qi, R. Lu, S. Wang, C. Xiang, C. Xie, M. Zheng, X. Tian, X. Xu, Selective fluorometric determination of microcystin-LR using a segment template molecularly imprinted by polymer-capped carbon quantum dots, Microchem. J. 161 (2021) 105798, https://doi.org/10.1016/j.microc.2020.105798.
[47] X.R. Wang, B.W. Li, H.Y. You, L.X. Chen, An ion imprinted polymers grafted paper-based fluorescent sensor based on quantum dots for detection of Cu^{2+} ions, Chin. J. Anal. Chem. 43 (2015) 1499–1504, https://doi.org/10.1016/S1872-2040(15)60867-2.
[48] J. Zhou, B. Li, A. Qi, Y. Shi, J. Qi, H. Xu, L. Chen, ZnSe quantum dot based ion imprinting technology for fluorescence detecting cadmium and lead ions on a three-dimensional rotary paper-based microfluidic chip, Sensor. Actuator. B Chem. 305 (2020), https://doi.org/10.1016/j.snb.2019.127462.
[49] M.Y. Zhang, R.F. Huang, X.G. Ma, L.H. Guo, Y. Wang, Y.M. Fan, Selective fluorescence sensor based on ion-imprinted polymer-modified quantum dots for trace detection of Cr(VI) in aqueous solution, Anal. Bioanal. Chem. 411 (2019) 7165–7175, https://doi.org/10.1007/s00216-019-02100-w.
[50] K. Chullasat, P. Nurerk, P. Kanatharana, F. Davis, O. Bunkoed, A facile optosensing protocol based on molecularly imprinted polymer coated on CdTe quantum dots for highly sensitive and selective amoxicillin detection, Sensor. Actuator. B Chem. 254 (2018) 255–263, https://doi.org/10.1016/j.snb.2017.07.062.
[51] H. Montaseri, P.B.C. Forbes, Analytical techniques for the determination of acetaminophen: a review, TrAC, Trends Anal. Chem. 108 (2018) 122–134, https://doi.org/10.1016/j.trac.2018.08.023.
[52] X. Xu, G. Xu, F. Wei, Y. Cen, M. Shi, X. Cheng, Y. Chai, M. Sohail, Q. Hu, Carbon dots coated with molecularly imprinted polymers: a facile bioprobe for fluorescent determination of caffeic acid, J. Colloid Interface Sci. 529 (2018) 568–574, https://doi.org/10.1016/j.jcis.2018.06.050.
[53] K. Chullasat, P. Kanatharana, O. Bunkoed, Nanocomposite optosensor of dual quantum dot fluorescence probes for simultaneous detection of cephalexin and ceftriaxone, Sensor. Actuator. B Chem. 281 (2019) 689–697, https://doi.org/10.1016/j.snb.2018.11.003.
[54] M. Fang, L. Zhou, H. Zhang, L. Liu, Z.Y. Gong, A molecularly imprinted polymers/carbon dots-grafted paper sensor for 3-monochloropropane-1,2-diol determination, Food Chem. 274 (2019) 156–161, https://doi.org/10.1016/j.foodchem.2018.08.133.
[55] L. Zheng, Y. Zheng, Y. Liu, S. Long, L. Du, J. Liang, C. Huang, M.T. Swihart, K. Tan, Core-shell quantum dots coated with molecularly imprinted polymer for selective photoluminescence sensing of perfluorooctanoic acid, Talanta 194 (2019) 1–6, https://doi.org/10.1016/j.talanta.2018.09.106.
[56] R. Shariati, B. Rezaei, H.R. Jamei, A.A. Ensafi, Application of coated green source carbon dots with silica molecularly imprinted polymers as a fluorescence probe

for selective and sensitive determination of phenobarbital, Talanta 194 (2019) 143–149, https://doi.org/10.1016/j.talanta.2018.09.069.
[57] T. Shi, L. Tan, H. Fu, J. Wang, Application of molecular imprinting polymer anchored on CdTe quantum dots for the detection of sulfadiazine in seawater, Mar. Pollut. Bull. 146 (2019) 591–597, https://doi.org/10.1016/j.marpolbul.2019.07.010.
[58] R. Long, T. Li, C. Tong, L. Wu, S. Shi, Molecularly imprinted polymers coated CdTe quantum dots with controllable particle size for fluorescent determination of p-coumaric acid, Talanta 196 (2019) 579–584, https://doi.org/10.1016/j.talanta.2019.01.007.
[59] M. Poshteh Shirani, B. Rezaei, A.A. Ensafi, A novel optical sensor based on carbon dots embedded molecularly imprinted silica for selective acetamiprid detection, Spectrochim. Acta Part A Mol. Biomol. Spectrosc. 210 (2019) 36–43, https://doi.org/10.1016/j.saa.2018.08.030.
[60] O. Bunkoed, P. Raksawong, R. Chaowana, P. Nurerk, A nanocomposite probe of graphene quantum dots and magnetite nanoparticles embedded in a selective polymer for the enrichment and detection of ceftazidime, Talanta 218 (2020) 121168, https://doi.org/10.1016/j.talanta.2020.121168.
[61] M. Masteri-Farahani, S. Mashhadi-Ramezani, N. Mosleh, Molecularly imprinted polymer containing fluorescent graphene quantum dots as a new fluorescent nanosensor for detection of methamphetamine, Spectrochim. Acta Part A Mol. Biomol. Spectrosc. 229 (2020) 118021, https://doi.org/10.1016/j.saa.2019.118021.
[62] J. Bai, L. Chen, Y. Zhu, X. Wang, X. Wu, Y. Fu, A novel luminescence sensor based on porous molecularly imprinted polymer-ZnS quantum dots for selective recognition of paclitaxel, Colloids Surfaces A Physicochem. Eng. Asp. 610 (2021) 125696, https://doi.org/10.1016/j.colsurfa.2020.125696.
[63] S. Chen, X. Su, C. Yuan, C.Q. Jia, Y. Qiao, Y. Li, L. He, L. Zou, X. Ao, A. Liu, S. Liu, Y. Yang, A magnetic phosphorescence molecularly imprinted polymers probe based on manganese-doped ZnS quantum dots for rapid detection of trace norfloxacin residual in food, Spectrochim. Acta Part A Mol. Biomol. Spectrosc. 253 (2021) 1–10, https://doi.org/10.1016/j.saa.2021.119577.
[64] Z. Dehghani, M. Akhond, G. Absalan, Carbon quantum dots embedded silica molecular imprinted polymer as a novel and sensitive fluorescent nanoprobe for reproducible enantioselective quantification of naproxen enantiomers, Microchem. J. 160 (2021) 105723, https://doi.org/10.1016/j.microc.2020.105723.
[65] R. Zhu, M. Lai, M. Zhu, H. Liang, Q. Zhou, R. Li, W. Zhang, H. Ye, A functional ratio fluorescence sensor platform based on the graphene/Mn-ZnS quantum dots loaded with molecularly imprinted polymer for selective and visual detection sinapic acid, Spectrochim. Acta Part A Mol. Biomol. Spectrosc. 244 (2021) 118845, https://doi.org/10.1016/j.saa.2020.118845.
[66] M. May, F. Chang, I.R. Ginjom, M. Ngu-schwemlein, Synthesis of yellow fluorescent carbon dots and their application to the determination of chromium (III) with selectivity improved by pH tuning, Microchim. Acta (2016) 1899–1907, https://doi.org/10.1007/s00604-016-1819-2.
[67] M. Cao, C. Cao, M. Liu, P. Wang, C. Zhu, Selective fluorometry of cytochrome c using glutathione-capped CdTe quantum dots in weakly basic medium, Microchim. Acta 165 (2009) 341–346, https://doi.org/10.1007/s00604-009-0140-8.
[68] F. Xu, H. Shi, X. He, K. Wang, D. He, L. Yan, X. Ye, J. Tang, J. Shangguan, L. Luo, Masking Agent-free and Channel-Switch-Mode Simultaneous Sensing of Fe3+ and Hg2+ Using Dual-Excitation Graphene Quantum Dots, 2015, pp. 3925–3928, https://doi.org/10.1039/c5an00468c.
[69] Y. Lou, J. Ji, A. Qin, L. Liao, Z. Li, S. Chen, K. Zhang, J. Ou, Functionalization for detection of metal ions. https://doi.org/10.1021/acsomega.0c00098, 2020.
[70] Y. Wu, Y. Liu, H. Liu, B. Liu, W. Chen, L. Xu, J. Liu, Ion-mediated self-assembly of Cys-capped quantum dots for fluorescence detection of As(III)in water, Anal. Methods (2020) 4229–4234, https://doi.org/10.1039/d0ay01144d.
[71] T. Gong, J. Liu, Y. Wu, Y. Xiao, X. Wang, S. Yuan, Fluorescence enhancement of CdTe quantum dots by HBcAb-HRP for sensitive detection of H_2O_2 in human serum, Biosens. Bioelectron. 92 (2017) 16–20, https://doi.org/10.1016/j.bios.2017.01.048.
[72] L. Zhang, C. Xu, B. Li, Simple and Sensitive Detection Method for Chromium (VI) in Water Using Glutathione — Capped CdTe Quantum Dots as Fluorescent Probes, 2009, pp. 61–68, https://doi.org/10.1007/s00604-009-0164-0.
[73] A.S. Lima, S.S.M. Rodrigues, M.G.A. Korn, D.S.M. Ribeiro, J.L.M. Santos, L.S. G. Teixeira, Determination of copper in biodiesel samples using CdTe-GSH quantum dots as photoluminescence probes, Microchem. J. 117 (2014) 144–148, https://doi.org/10.1016/j.microc.2014.06.021.
[74] H. Wu, J. Liang, H. Han, A novel method for the determination of Pb^{2+} based on the quenching of the fluorescence of CdTe quantum dots, Microchim. Acta 161 (2008) 81–86, https://doi.org/10.1007/s00604-007-0801-4.
[75] Y. Zhang, H. Zhang, X. Guo, H. Wang, L-Cysteine-coated CdSe/CdS Core-Shell Quantum Dots as Selective Fluorescence Probe for Copper (II) Determination, vol. 89, 2008, pp. 142–147, https://doi.org/10.1016/j.microc.2008.01.008.
[76] A. Başoğlu, Ü. Ocak, A. Gümrükçüoğlu, Synthesis of microwave-assisted fluorescence carbon quantum dots using roasted – chickpeas and its applications for sensitive and selective detection of Fe^{3+} ions, J. Fluoresc. (2020) 515–526.
[77] L. Xi, H. Ma, G. Tao, Thiourea functionalized CdSe/CdS quantum dots as a fluorescent sensor for mercury ion detection, Chin. Chem. Lett. 27 (2016) 1531–1536, https://doi.org/10.1016/j.cclet.2016.03.002.
[78] L.G. Benzi, M.G.A. Korn, R.M.M. Santana, Capped cadmium telluride quantum dots fluorescence enhancement by Se(IV) and its application to dietary supplements analysis, Chem. Phys. Lett. 771 (2021), https://doi.org/10.1016/j.cplett.2021.138526.
[79] Q. Liu, Y. Lin, J. Xiong, L. Wu, X. Hou, K. Xu, C. Zheng, Disposable paper-based analytical device for visual speciation analysis of Ag(I) and silver nanoparticles (AgNPs), Anal. Chem. 91 (2019) 3359–3366, https://doi.org/10.1021/acs.analchem.8b04609.
[80] J. Proch, P. Niedzielski, In – spray chamber hydride generation by multi – mode sample introduction system (MSIS) as an interface in the hyphenated system of high performance liquid chromatography and inductivity coupled plasma optical emission spectrometry (HPLC/HG–ICP –OES, Talanta 208 (2020) 120395, https://doi.org/10.1016/j.talanta.2019.120395.
[81] P. Hu, X. Wang, Z. Wang, R. Dai, W. Deng, H. Yu, K. Huang, Trends in Analytical Chemistry Recent developments of hydride generation in non-atomic spectrometric methods, Trends Anal. Chem. 119 (2019) 115617, https://doi.org/10.1016/j.trac.2019.07.028.
[82] Z. Long, Y. Luo, C. Zheng, P. Deng, X. Hou, Recent dvance of hydride generation-analytical atomic spectrometry: Part I-technique development, Appl. Spectrosc. Rev. 47 (2012) 382–413, https://doi.org/10.1080/05704928.2012.666775.
[83] N. Butwong, S. Srijaranai, W. Ngeontae, R. Burakham, Speciation of arsenic (III) and arsenic (V) based on quenching of CdS quantum dots fluorescence using hybrid sequential injection-stopped flow injection gas-diffusion system, Spectrochim. Acta Part A Mol. Biomol. Spectrosc. 97 (2012) 17–23, https://doi.org/10.1016/j.saa.2012.05.054.
[84] I. Costas-Mora, V. Romero, F. Pena-Pereira, I. Lavilla, C. Bendicho, Quantum dot-based headspace single-drop microextraction technique for optical sensing of volatile species, Anal. Chem. 83 (2011) 2388–2393, https://doi.org/10.1021/ac103223e.
[85] I. Costas-Mora, V. Romero, F. Pena-Pereira, I. Lavilla, C. Bendicho, Quantum dots confined in an organic drop as luminescent probes for detection of selenium by microfluorospectrometry after hydridation: study of the quenching mechanism and analytical performance, Anal. Chem. 84 (2012) 4452–4459, https://doi.org/10.1021/ac300221s.
[86] C. Carrillo-Carrión, B.M. Simonet, M. Valcárcel, (CdSe/ZnS QDs)-ionic liquid-based headspace single drop microextraction for the fluorimetric determination of trimethylamine in fish, Analyst 137 (2012) 1152–1159, https://doi.org/10.1039/c2an15914g.
[87] K. Huang, K. Xu, W. Zhu, L. Yang, X. Hou, C. Zheng, Hydride generation for headspace solid-phase extraction with CdTe quantum dots immobilized on paper for sensitive visual detection of selenium, Anal. Chem. 88 (2016) 789–795, https://doi.org/10.1021/acs.analchem.5b03128.
[88] J. Xiong, K. Xu, X. Hou, P. Wu, AuNCs-catalyzed hydrogen selenide oxidation: mechanism and application for headspace fluorescent detection of Se(IV), Anal. Chem. 91 (2019) 6141–6148, https://doi.org/10.1021/acs.analchem.9b00738.
[89] K. Huang, R. Dai, W. Deng, S. Guo, H. Deng, Y. Wei, F. Zhou, Y. Long, J. Li, X. Yuan, X. Xiong, Gold nanoclusters immobilized paper for visual detection of zinc in whole blood and cells by coupling hydride generation with headspace solid phase extraction, Sensor. Actuator. B Chem. 255 (2018) 1631–1639, https://doi.org/10.1016/j.snb.2017.08.177.
[90] K. Huang, R. Dai, W. Deng, L. Lin, A. Zhang, X. Yuan, Aqueous synthesis of CdTe quantum dots by hydride generation for visual detection of silver on quantum dot immobilized paper, Anal. Methods 9 (2017) 5339–5347, https://doi.org/10.1039/c7ay01705g.
[91] O. Thepmanee, K. Prapainop, O. Noppha, N. Rattanawimanwong, W. Siangproh, O. Chailapakul, K. Songsrirote, A simple paper-based approach for arsenic determination in water using hydride generation coupled with mercaptosuccinic-acid capped CdTe quantum dots, Anal. Methods 12 (2020) 2718–2726, https://doi.org/10.1039/d0ay00273a.
[92] S. Benítez-Martínez, Á.I. López-Lorente, M. Valcárcel, Determination of TiO2 nanoparticles in sunscreen using N-doped graphene quantum dots as a fluorescent probe, Microchim. Acta 183 (2016) 781–789, https://doi.org/10.1007/s00604-015-1696-0.
[93] S. Feng, Z. Mu, H. Liu, J. Huang, X. Li, Y. Yang, A novel application of fluorine doped carbon dots combining vortex-assisted liquid-liquid microextraction for determination of 4-nitrophenol with spectrofluorimetric method, J. Fluoresc. 29 (2019) 1133–1141, https://doi.org/10.1007/s10895-019-02427-8.
[94] Z. Xu, C. Zhang, X. Yu, H. Zheng, L. Xu, Microwave-assisted Solid-phase Synthesis of Nitrogen-Doping Carbon Dot with Good Solvent Compatibility and its Sensing of Sunitinib, 2021, pp. 6435–6447.
[95] I. Costas-Mora, V. Romero, I. Lavilla, C. Bendicho, Solid-state chemiluminescence assay for ultrasensitive detection of antimony using on-vial immobilization of CdSe quantum dots combined with liquid-liquid-liquid microextraction, Anal. Chim. Acta 788 (2013) 114–121, https://doi.org/10.1016/j.aca.2013.06.007.
[96] Z. Saeedi, A. Lotfi, J. Hassanzadeh, N. Nafiseh Bagheri, High sensitive determination of copper (II) ions using fluorescence and chemiluminescence emissions of modified CdS quantum dots after it's preconcentration by dispersive, Psychol. Appl. to Work An Introd. to Ind. Organ. Psychol. Tenth Ed. Paul 53 (2012) 1689–1699, https://doi.org/10.1017/CBO9781107415324.004.
[97] I. Costas-mora, V. Romero, F. Pena-pereira, I. Lavilla, C. Bendicho, Quantum dot-based headspace single-drop microextraction technique for optical sensing of volatile species, Anal. Chem. 83 (2011) 2388–2393.
[98] E. Jafarnejad, J. Abolhasani, A. Derakhshan, Pre-concentration and determination of fluorescence quenching of CdS quantum dots of Pb ions by dispersive liquid–liquid microextraction in the presence of the ionic liquids, Pigment Resin, Technol. 47 (2018) 127–132, https://doi.org/10.1108/prt-11-2015-0115.
[99] C.F. Poole, New trends in solid-phase extraction, TrAC, Trends Anal. Chem. 22 (2003) 362–373, https://doi.org/10.1016/S0165-9936(03)00605-8.

[100] J. Płotka-Wasylka, N. Szczepańska, M. de la Guardia, J. Namieśnik, Modern trends in solid phase extraction: new sorbent media, TrAC, Trends Anal. Chem. 77 (2016) 23–43, https://doi.org/10.1016/j.trac.2015.10.010.
[101] A. Andrade-Eiroa, M. Canle, V. Leroy-Cancellieri, V. Cerdà, Solid-phase extraction of organic compounds: a critical review (Part I), TrAC, Trends Anal. Chem. 80 (2016) 641–654, https://doi.org/10.1016/j.trac.2015.08.015.
[102] L. Lu, R. Zeng, Q. Lin, X. Huang, D. Tang, Cation exchange reaction-mediated photothermal and polarity-switchable photoelectrochemical dual-readout biosensor, Anal. Chem. 95 (2023) 16335–16342, https://doi.org/10.1021/acs.analchem.3c03573.
[103] R. Zeng, K. Lian, B. Su, L. Lu, J. Lin, D. Tang, S. Lin, X. Wang, Versatile synthesis of hollow metal sulfides via reverse cation exchange reactions for photocatalytic CO2 reduction, Angew. Chem. Int. Ed. 60 (2021) 25055–25062, https://doi.org/10.1002/anie.202110670.
[104] C.A.T. Toloza, S. Khan, R.L.D. Silva, E.C. Romani, D.G. Larrude, S.R.W. Louro, F. L. Freire, R.Q. Aucélio, Photoluminescence suppression effect caused by histamine on amino-functionalized graphene quantum dots with the mediation of Fe^{3+}, Cu^{2+}, Eu^{3+}: application in the analysis of spoiled tuna fish, Microchem. J. 133 (2017) 448–459, https://doi.org/10.1016/j.microc.2017.04.013.
[105] M.S. Hosseini, S. Nazemi, Preconcentration determination of arsenic species by sorption of As(v) on Amberlite IRA-410 coupled with fluorescence quenching of l-cysteine capped CdS nanoparticles, Analyst 138 (2013) 5769–5776, https://doi.org/10.1039/c3an00869j.
[106] M. Park, H.D. Ha, Y.T. Kim, J.H. Jung, S.H. Kim, D.H. Kim, T.S. Seo, Combination of a sample pretreatment microfluidic device with a photoluminescent graphene oxide quantum dot sensor for trace lead detection, Anal. Chem. 87 (2015) 10969–10975, https://doi.org/10.1021/acs.analchem.5b02907.
[107] X. Xu, Z. Chen, Q. Li, D. Meng, H. Jiang, Y. Zhou, S. Feng, Y. Yang, Copper and nitrogen-doped carbon dots as an anti-interference fluorescent probe combined with magnetic material purification for nicotine detection, Microchem. J. 160 (2021) 105708, https://doi.org/10.1016/j.microc.2020.105708.
[108] J. Hua, Y. Jiao, M. Wang, Y. Yang, Determination of norfloxacin or ciprofloxacin by carbon dots fluorescence enhancement using magnetic nanoparticles as adsorbent, Microchim. Acta 185 (2018) 1–9, https://doi.org/10.1007/s00604-018-2685-x.
[109] M.H. Costa, D.T.S. Ferreira, J.E.S. Pádua, J.P.A. Fernandes, J.C.C. Santos, F.A. S. Cunha, M.C.U. Araujo, A fast, low-cost, sensitive, selective, and non-laborious method based on functionalized magnetic nanoparticles, magnetic solid-phase extraction, and fluorescent carbon dots for the fluorimetric determination of copper in wines without prior sample treatment, Food Chem. 363 (2021), https://doi.org/10.1016/j.foodchem.2021.130248.
[110] S. Han, X. Li, Y. Wang, C. Su, A core-shell Fe3O4 nanoparticle-CdTe quantum dot-molecularly imprinted polymer composite for recognition and separation of 4-nonylphenol, Anal. Methods 6 (2014) 2855–2861, https://doi.org/10.1039/c3ay41924j.
[111] H. Zheng, R. Su, Z. Gao, W. Qi, R. Huang, L. Wang, Z. He, Magnetic-fluorescent nanocomposites as reusable fluorescence probes for sensitive detection of hydrogen peroxide and glucose, Anal. Methods 6 (2014) 6352–6357, https://doi.org/10.1039/c4ay00886c.
[112] A. Saha, T. Debnath, S. Neogy, H.N. Ghosh, M.K. Saxena, B.S. Tomar, Micellar extraction assisted fluorometric determination of ultratrace amount of uranium in aqueous samples by novel diglycolamide-capped quantum dot nanosensor, Sensor. Actuator. B Chem. 253 (2017) 592–602, https://doi.org/10.1016/j.snb.2017.06.171.
[113] K. Takemura, J. Lee, T. Suzuki, T. Hara, F. Abe, E.Y. Park, Ultrasensitive detection of norovirus using a magnetofluoroimmunoassay based on synergic properties of gold/magnetic nanoparticle hybrid nanocomposites and quantum dots, Sensor. Actuator. B Chem. 296 (2019) 126672, https://doi.org/10.1016/j.snb.2019.126672.
[114] M. Park, T.S. Seo, An integrated microfluidic device with solid-phase extraction and graphene oxide quantum dot array for highly sensitive and multiplex detection of trace metal ions, Biosens. Bioelectron. 126 (2019) 405–411, https://doi.org/10.1016/j.bios.2018.11.010.
[115] M. Wang, M. Gao, L. Deng, X. Kang, K. Zhang, Q. Fu, Z. Xia, D. Gao, A sensitive and selective fluorescent sensor for 2,4,6-trinitrophenol detection based on the composite material of magnetic covalent organic frameworks, molecularly imprinted polymers and carbon dots, Microchem. J. 154 (2020) 104590, https://doi.org/10.1016/j.microc.2019.104590.
[116] M. Gagic, L. Nejdl, K. Xhaxhiu, N. Cernei, O. Zitka, E. Jamroz, P. Svec, L. Richtera, P. Kopel, V. Milosavljevic, V. Adam, Fully automated process for histamine detection based on magnetic separation and fluorescence detection, Talanta 212 (2020) 120789, https://doi.org/10.1016/j.talanta.2020.120789.
[117] A.B. Ganganboina, A.D. Chowdhury, I.M. Khoris, R. an Doong, T.C. Li, T. Hara, F. Abe, T. Suzuki, E.Y. Park, Hollow magnetic-fluorescent nanoparticles for dual-modality virus detection, Biosens. Bioelectron. 170 (2020) 112680, https://doi.org/10.1016/j.bios.2020.112680.
[118] R.C. Castro, M.L.M.F.S. Saraiva, J.L.M. Santos, D.S.M. Ribeiro, Multiplexed detection using quantum dots as photoluminescent sensing elements or optical labels, Coord. Chem. Rev. 448 (2021) 214181, https://doi.org/10.1016/j.ccr.2021.214181.
[119] A.C. Olivieri, Chemometrics and multivariate calibration, Introd. to Multivar. Calibration (2018) 1–17, https://doi.org/10.1007/978-3-319-97097-4_1.
[120] G.M. Escandar, H.C. Goicoechea, A. Mu, Second- and higher-order data generation and calibration : a tutorial, Anal. Chim. Acta 806 (2014) 8–26, https://doi.org/10.1016/j.aca.2013.11.009.
[121] A.C. Olivieri, Analytical advantages of multivariate data processing. One, two, three, infinity? Anal. Chem. 80 (2008) 5713–5720, https://doi.org/10.1021/ac800692c.
[122] D.B. Bittar, D.S.M. Ribeiro, R.N.M.J. Páscoa, J.X. Soares, S.S.M. Rodrigues, R. C. Castro, L. Pezza, H.R. Pezza, J.L.M. Santos, Multiplexed analysis combining distinctly-sized CdTe-MPA quantum dots and chemometrics for multiple mutually interfering analyte determination, Talanta 174 (2017) 572–580, https://doi.org/10.1016/j.talanta.2017.06.071.
[123] D.S.M. Ribeiro, R.C. Castro, R.N.M.J. Páscoa, J.X. Soares, Tuning CdTe quantum dots reactivity for multipoint detection of mercury (II), silver (I) and copper (II), J. Lumin. 207 (2019) 386–396, https://doi.org/10.1016/j.jlumin.2018.11.035.
[124] R.C. Castro, D.S.M. Ribeiro, R.N.M.J. Páscoa, J.X. Soares, S.J. Mazivila, J.L. M. Santos, Dual-emission CdTe/$AgInS_2$ photoluminescence probe coupled to neural network data processing for the simultaneous determination of folic acid and iron (II), Anal. Chim. Acta 1114 (2020) 29–41, https://doi.org/10.1016/j.aca.2020.04.007.
[125] A. Barati, M. Shamsipur, H. Abdollahi, Hybrid of non-selective quantum dots for simultaneous determination of TNT and 4-nitrophenol using multivariate chemometrics methods, Anal. Methods 6 (2014) 6577–6584, https://doi.org/10.1039/c4ay01326c.
[126] H. Abdollahi, M. Shamsipur, A. Barati, Kinetic fluorescence quenching of CdS quantum dots in the presence of Cu (II): chemometrics-assisted resolving of the kinetic data and quantitative analysis of Cu (II), Spectrochim. ACTA PART A Mol. Biomol. Spectrosc. 127 (2014) 137–143, https://doi.org/10.1016/j.saa.2014.02.020.
[127] R.C. Castro, R.N.M.J. Páscoa, M.L.M.F.S. Saraiva, J.L.M. Santos, D.S.M. Ribeiro, Chemometric-assisted kinetic determination of oxytetracycline using $AgInS_2$ quantum dots as PL sensing platforms, Anal. Chim. Acta 1188 (2021), https://doi.org/10.1016/j.aca.2021.339174.
[128] J.M.M. Leitão, H. Gonçalves, C. Mendonça, J.C.G. Esteves da Silva, Multiway chemometric decomposition of EEM of fluorescence of CdTe quantum dots obtained as function of pH, Anal. Chim. Acta 628 (2008) 143–154, https://doi.org/10.1016/j.aca.2008.09.020.
[129] P. Mishra, J. Roger, D. Jouan-rimbaud-bouveresse, A. Biancolillo, F. Marini, A. Nordon, D.N. Rutledge, Recent trends in multi-block data analysis in chemometrics for multi- source data integration, Trends Anal. Chem. 137 (2021) 116206, https://doi.org/10.1016/j.trac.2021.116206.
[130] Z. Sun, H.H. Xing, M. Qing, Y. Shi, Y. Ling, N.B. Li, H.Q. Luo, From the perspective of high-throughput recognition : sulfur quantum dots-based multi-channel sensing platform for metal ions detection, Chem. Eng. J. 452 (2023) 139594, https://doi.org/10.1016/j.cej.2022.139594.